

See discussions, stats, and author profiles for this publication at: <https://www.researchgate.net/publication/266253231>

# Synthesis, characterization, DFT calculation and biological activity of square-planar Ni(II) complexes with tridentate PNO ligands and monodentate pseudohalides. Part II

ARTICLE *in* EUROPEAN JOURNAL OF MEDICINAL CHEMISTRY · SEPTEMBER 2014

Impact Factor: 3.45 · DOI: 10.1016/j.ejmech.2014.06.079 · Source: PubMed

---

CITATIONS

2

---

READS

116

## 13 AUTHORS, INCLUDING:



[Sinisa Radulovic](#)

Institut za onkologiju i radiologiju Srbije

199 PUBLICATIONS 1,845 CITATIONS

[SEE PROFILE](#)



[Marcel Swart](#)

Catalan Institution for Research and Advanc...

153 PUBLICATIONS 3,359 CITATIONS

[SEE PROFILE](#)

# Accepted Manuscript

Synthesis, characterization, DFT calculation and biological activity of square-planar Ni(II) complexes with tridentate PNO ligands and monodentate pseudohalides. Part II

Milica Milenković, Andrej Pevec, Iztok Turel, Miroslava Vujčić, Marina Milenković, Katarina Jovanović, Nevenka Gligorijević, Siniša Radulović, Marcel Swart, Maja Gruden-Pavlović, Kawther Adaila, Božidar Čobeljić, Katarina Andelković



PII: S0223-5234(14)00882-4

DOI: [10.1016/j.ejmech.2014.06.079](https://doi.org/10.1016/j.ejmech.2014.06.079)

Reference: EJMECH 7370

To appear in: *European Journal of Medicinal Chemistry*

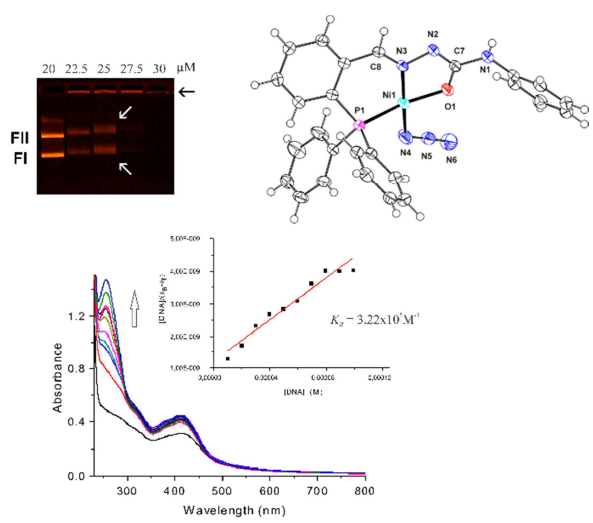
Received Date: 8 April 2014

Revised Date: 10 June 2014

Accepted Date: 12 June 2014

Please cite this article as: M. Milenković, A. Pevec, I. Turel, M. Vujčić, M. Milenković, K. Jovanović, N. Gligorijević, S. Radulović, M. Swart, M. Gruden-Pavlović, K. Adaila, B. Čobeljić, K. Andelković, Synthesis, characterization, DFT calculation and biological activity of square-planar Ni(II) complexes with tridentate PNO ligands and monodentate pseudohalides. Part II, *European Journal of Medicinal Chemistry* (2014), doi: 10.1016/j.ejmech.2014.06.079.

This is a PDF file of an unedited manuscript that has been accepted for publication. As a service to our customers we are providing this early version of the manuscript. The manuscript will undergo copyediting, typesetting, and review of the resulting proof before it is published in its final form. Please note that during the production process errors may be discovered which could affect the content, and all legal disclaimers that apply to the journal pertain.



**Synthesis, characterization, DFT calculation and biological activity of square-planar Ni(II) complexes with tridentate PNO ligands and monodentate pseudohalides. Part II.**

Milica Milenković<sup>a</sup>, Andrej Pevec<sup>b</sup>, Iztok Turel<sup>b</sup>, Miroslava Vujčić<sup>c</sup>, Marina Milenković<sup>d</sup>, Katarina Jovanović<sup>e</sup>, Nevenka Gligorijević<sup>e</sup>, Siniša Radulović<sup>e</sup>, Marcel Swart<sup>f,g</sup>, Maja Gruden-Pavlović<sup>a</sup>, Kawther Adaila<sup>a</sup>, Božidar Čobeljić<sup>a</sup> and Katarina Andelković<sup>a</sup><sup>1</sup>

<sup>a</sup>*Faculty of Chemistry, University of Belgrade, Studentski trg 12–16, 11000 Belgrade, Serbia*

<sup>b</sup>*Faculty of Chemistry and Chemical Technology, University of Ljubljana, Aškerčeva 5, 1000 Ljubljana, Slovenia*

<sup>c</sup>*Institute of Chemistry, Technology and Metallurgy, University of Belgrade, Njegoševa 12, P.O. Box 815, 11000 Belgrade, Serbia*

<sup>d</sup>*Department of Microbiology and Immunology, Faculty of Pharmacy, University of Belgrade, Vojvode Stepe 450, Serbia*

<sup>e</sup>*Institute for Oncology and Radiology of Serbia, Department of Experimental Oncology, Laboratory for Experimental Pharmacology, Pasterova 14, Belgrade, Serbia*

<sup>f</sup>*Institució Catalana de Recerca i Estudis Avançats (ICREA), Pg. Lluís Companys 23, 08010 Barcelona, Spain*

<sup>g</sup>*Institut de Química Computacional i Catàlisi and Departament de Química, Universitat de Girona, Campus Montilivi, 17071 Girona, Spain*

## Abstract

Three square-planar complexes of Ni(II) with condensation derivative of 2-(diphenylphosphino)benzaldehyde and 4-phenylsemicarbazide and monodentate pseudohalides have been synthesized and characterized on the basis of the results of X-ray, NMR and IR spectroscopy and elemental analysis. Investigated complexes exhibited moderate antibacterial and cytotoxic activity. The most pronounced cytotoxic activity (in the

---

<sup>1</sup> Corresponding author. Tel.: +381 11 3282 750.  
E-mail address: kka@chem.bg.ac.rs (K. Andelković).

range of cisplatin) to HeLa cell line was observed for ligand and all the complexes. Azido complex and ligand induced concentration dependent cell cycle arrest in the S phase, as well as decrease of percentage of cells in G1 phase, without significant increase of apoptotic fraction of cells. The interaction of the azido complex and ligand with CT-DNA results in changes in UV-Vis spectra typical for non-covalent bonding. The observed intrinsic binding constant of azido complex-CT-DNA and ligand-CT-DNA were  $3.22 \times 10^5 \text{ M}^{-1}$  and  $2.79 \times 10^5 \text{ M}^{-1}$ . The results of DNA cleavage experiments showed that azido complex nicked supercoiled plasmid DNA.

**Keywords:** Nickel(II) complexes, Pseudohalides, X-ray crystal structures, Antimicrobial activity, Cytotoxicity

## 1. Introduction

The discovery of anticancer properties of auranofin [1-(thio- $\kappa$ S)- $\beta$ -D-glucopyranose-2,3,4,6-tetraacetato](triethylphosphine)gold triggered research on the synthesis and biological activity examination of metal complexes with different phosphine ligands with the stress on their antitumor activity [1–5]. Moreover the investigation of pharmacological activity of hydrazones demonstrated that this class of compounds possess also antidepressant, anticonvulsant, analgesic, antiinflammatory, antimicrobial, antimalarial and antitumor activities [6]. Having these facts in mind we directed our attention towards the synthesis, characterization and biological activity evaluation of hydrazone derivatives of 2-(diphenylphosphino)benzaldehyde and corresponding metal complexes [7–11]. Recently, we synthesized condensation derivative of 2-(diphenylphosphino)benzaldehyde and ethyl carbamate [9–11] and our focus was on the coordination and biological chemistry. With this ligand we synthesized three square-planar Ni(II) complexes with tridentate PNO coordinated phosphine ligand and different monodentate pseudohalides (cyanate, thiocyanate and azide, respectively) in the fourth coordination place and studied their antimicrobial and antitumor activities. Examination of biological activity of Ni(II) complexes showed that the activity depends on the nature of monodentate ligand. Antifungal activity of all the complexes was stronger than the activity of ligand, while only the azido complex had an antibacterial activity. The results of cytotoxic activity demonstrated that all the

complexes showed activity to all investigated cell lines (six tumor cell lines (A549, MDA-MB-361, HeLa, FemX, LS-174 and K562) and one normal cell line (MRC-5)) and were more active than the ligand. Cytotoxic activity of all the complexes was the most pronounced on leukemia cell line K562. Among the complexes, azido complex showed the strongest activity to this cell line which was similar to cisplatin activity. The azido complex was the most cytotoxic to K562 and MDA-MB-361 cells, isothiocyanato complex for LS-174 cell line, and cyanato for normal MRC-5 cells, while for the other cell lines no significant difference could be seen. The investigated complexes induced perturbations of cell cycle of HeLa cells (increase of percentage of cells in sub-G1 phase and decrease of percentage of cells in G1 phase) and DNA damage [11]. According to the results of biological activity we proposed that the non-electrolyte nature of the lipophilic complexes might facilitate transport of nickel and pseudohalides through biological membranes.

In this study, we described the synthesis, characterization, DFT calculations and biological activity evaluation of the three square-planar nickel(II) complexes of the general formula  $[\text{NiLX}]$  ( $\mathbf{L}$  = 2-(diphenylphosphino)benzaldehyde 4-phenyl semicarbazone [12], X =  $\text{NCO}^-$  (**1**),  $\text{NCS}^-$  (**2**) and  $\text{N}_3^-$  (**3**)). The main differences between these two series of Ni(II) complexes that could affect biological activity are lipophilicity of complexes (aromatic ring instead of ethyl group), metabolic stability of hydrazone ligand (amide instead of ester group) and the influence of electronic distribution in molecule of complex on substitution rates of monodentate ligands.

## 2. Results and discussion

### 2.1. Synthesis

The ligand 2-(diphenylphosphino)benzaldehyde 4-phenylsemicarbazone (**HL**) was prepared using previously described procedure [12]. The ligand was used for preparation of complexes labeled **1**, **2** and **3**, Scheme 1.

The monoanionic enol tautomer of ligand was coordinated as tridentate via phosphorus, imine nitrogen and carbonyl oxygen atoms, while the fourth coordination place was occupied by monodentate cyanate, thiocyanate or azide group, respectively.

<Scheme 1.>

## 2.2. *Description of the crystal structures*

Crystals of products **1–3** suitable for X-ray analyses were prepared by slow evaporation of solvent at room temperature. Selected bond lengths and angles are given in Table 1. The structure of all three complexes **1–3** possess the tridentate semicarbazone ligand **L** coordinated to the nickel atom with a PNO set of donor atoms forming one five-membered and one six-membered chelate ring. The structure of compounds **1–3** are displayed in Figures 1–3. The cyanate (**1**), thiocyanate (**2**) and azide (**3**) nitrogen atom completes the square-planar coordination mode of nickel atom in the corresponding complexes. The coordination squares in complexes **1–3** are distorted as is confirmed by the given interatomic bond angles stated in Table 1. The sum of the nickel-containing angles in complexes **1–3** is about 360°. The largest deviation from the best plane that contained the coordination sphere is found for carboxyl O1 atom in all three complexes **1–3**. The values are 0.0983(6), 0.1229(19) and 0.2046(10) Å out of the plane for **1**, **2**, and **3**, respectively. The angle in pseudohalide ligands are close to the linearity (Table 1), but the coordination angle differs from **1** to **3**. The angles Ni1–N4–C27 in **1** and **2** are close to each other (164.90(16)° and 161.2(4)°, respectively), but in the case of **3** the angle Ni1–N4–N5 significantly deviate from linearity (120.73(18)°). This value is also in accordance to the Ni–N<sub>3</sub> moieties in similar Ni complex found in literature [11]. The bond lengths for the coordination sphere in **1–3** are comparable to those found in other square-planar complexes for nickel(II) [13–17]. To the best of our knowledge, only a one example of the ligand **L** coordinated to the metallic center was structurally characterized with the unusual coordination of the semicarbazone ligand via the amido nitrogen atom to the rhenium atom [12].

<**Fig. 1.**>

<Fig. 2.>

<Fig. 3.>

Intermolecular interactions that exist in the solid state of compounds **1–3** are depicted in Figures S1–S3 (Supplementary Material). N-H···O in **1** and N-H···S hydrogen bonds in **2** connect the molecules, producing an infinite chain. The hydrogen bonds are formed between amide nitrogen atom and cyanato oxygen or thiocyanato sulphur atom as an acceptor atom in **1** and **2**, respectively. Contrary, in compound **3** two complex molecules are stabilized by a pair of intermolecular N-H···N contacts between azido nitrogen and N<sub>2</sub> atom as an acceptor of weak interaction. Possible non-covalent interactions are listed in Table 2.

<Table 1>

<Table 2>

### 2.3. IR spectra

Coordination of the ligand (**HL**) to the Ni(II) caused the bathochromical shift of bands which correspond to the vibrations of carbonyl (1682 cm<sup>-1</sup> for **HL**, 1537 cm<sup>-1</sup> for complex **1**, 1533 cm<sup>-1</sup> for complex **2** and 1539 cm<sup>-1</sup> for complex **3**) and azomethine groups (1597 cm<sup>-1</sup> for **HL**, 1503 cm<sup>-1</sup> for complex **1**, 1499 cm<sup>-1</sup> for complex **2** and 1491 cm<sup>-1</sup> for complex **3**) of the ligand. The position of the band corresponding to  $\nu$ (C–P) vibrations is constant in the IR spectra of complexes as well as ligand (1438 cm<sup>-1</sup> in the spectrum of **HL**, 1438 cm<sup>-1</sup> in the spectrum of **1**, 1436 cm<sup>-1</sup> in the spectrum of **2**, 1439 cm<sup>-1</sup> in the spectrum of **3**). Coordination of the monodentate pseudohalides can be additionally confirmed from the appearance of a new band in the IR spectra of complexes at 2251 cm<sup>-1</sup> in the spectrum of **1** due to coordinated cyanate ion, at 2107 cm<sup>-1</sup> in the spectrum of **2** due to coordinated thiocyanate ion and at 2034 cm<sup>-1</sup> in the spectrum of **3** due to coordinated azide ion.

## 2.4. NMR spectra

### 2.4.1. $^1\text{H}$ NMR spectra

The signal of hydrazide NH1 observed at 10.84 ppm in the  $^1\text{H}$  NMR spectrum of free **HL** ligand is absent in the  $^1\text{H}$  NMR spectra of complexes **1–3**, indicating that the ligand is coordinated in monodeprotonated form (Table 3). Coordination via the imine nitrogen can be clearly seen from the  $^1\text{H}$  NMR spectra of complexes from the position of the signal of the hydrogen at C1 atom which is shifted upfield in comparison to the corresponding signal in the ligand. In the  $^1\text{H}$  NMR spectra of complexes **1–3** signals of most aromatic protons from the phosphino part of ligand are shifted downfield, suggesting that coordination occurs via phosphorus atom. Upon coordination of the ligand chemical shifts of aromatic protons from the amide part of the ligand as well as from hydrogen atom NH2 are shifted upfield indicating that resonance effect had important influence on electron distribution in complexes.

<Table 3>

### 2.4.2. $^{13}\text{C}$ NMR spectra

From the  $^{13}\text{C}$  NMR spectra of complexes **1–3** (Table 4) it can be seen that coordination through the imine nitrogen atom results in a downfield shift of the azomethine carbon C1. The signals of carbon atoms directly bound to the phosphorus are shifted strongly upfield indicating that the phosphorus atom is involved in coordination. The coordination via phosphorus atom results in electron withdrawal of aromatic carbon atoms which signals are shifted downfield. There is a strong downfield shift of the carbonyl carbon C16 which is the consequence of coordination of carbonyl oxygen atom to Ni(II). The insignificant changes in the position of signals of aromatic carbon atoms from the amide part of the ligand suggests that the amide nitrogen atom is not involved in the coordination.

<Table 4>

## 2.5 Computational studies

The DFT optimized structures of the investigated complexes are in excellent agreement with the X-ray structures. All three complexes showed distorted square planar coordination around  $\text{Ni}^{2+}$  ion with the semicarbazone ligand **L** coordinated as tridentate, and cyanate, thiocyanate and azide, respectively, coordinated via nitrogen as monodentate ligand. Since for similar systems [11] the ambidentate NCO ligand was bound to the nickel via oxygen, we have explored possible isomerism, and found that Ni-N coordination is favored in all cases (by 17.0  $\text{kcal}\cdot\text{mol}^{-1}$  for NCO vs. OCN, and 4.3  $\text{kcal}\cdot\text{mol}^{-1}$  for NCS vs. SCN; all data obtained at OPBE/TZ2P level, see Supplementary Material for molecular energies and Cartesian coordinates). The results follow the same trends irrespective of the environment (vacuum or solvent).

## 2.6. Antimicrobial activity

The results of antimicrobial activity of ligand **HL** and three Ni(II) complexes are presented in Table 5. Complex **3** showed moderate antibacterial activity on Gram-negative bacteria, while the activities of complexes **1** and **2** were weak. Moderate activities of the complexes were observed on most of the tested Gram-positive bacteria. The maximum activity against *Candida albicans* was observed for ligand itself.

Comparison of antimicrobial activity results for Ni(II) complexes of 2-(diphenylphosphino)benzaldehyde 4-phenylsemicarbazone with previously examined antimicrobial activity of Ni(II) complexes with condensation product of 2-(diphenylphosphino)benzaldehyde and ethyl carbazole [11] provide insights into structure-activity relationship. The presence of amide instead of ester group and aromatic ring instead of ethyl group in phosphine ligand results in enhanced antibacterial activity. Differences in antibacterial activity of two series of Ni(II) complexes could be results of more lipophilic nature and improved resistance to hydrolysis of 2-(diphenylphosphino)benzaldehyde 4-phenylsemicarbazone ligand. The most pronounced antibacterial activity for both of the series of Ni(II) complexes was observed for complexes with azido ligand in the fourth coordination

place. Selectivity of Ni(II) complexes to specific bacterial strains depends on the nature of monodentate ligand. Both of the tridentate PNO ligand molecules showed antifungal activity so the phosphine hydrazone part of the molecule is probably responsible for antifungal activity.

**<Table 5>**

### 2.7. MTT assay

Cytotoxic activity of investigated compounds and cisplatin (CDDP) as standard cytotoxic metal based agent, was determined by MTT assay after 48 h treatment of six tumour cell lines (HeLa, A549, FemX, LS-174, MDA-MB-453, K562) and one normal cell line (MRC-5). Results are shown in Table 6 in terms of IC<sub>50</sub> values for 48 h incubation period. IC<sub>50</sub> values are calculated as mean values obtained from two to three independent experiments and presented with their standard deviations.

**<Table 6>**

Results of this assay indicate that all investigated nickel complexes (**1–3**) showed moderate cytotoxic activity in all tumour cell lines, except in HeLa cells, where cytotoxicity was in the range of cisplatin. Regarding the lower sensitivity of A549 cell line to treatments in general, it is worth mentioning that A549 cells exhibited higher sensitivity to all four nickel complexes in comparison to other tumour cell lines, which is a promising result.

Ligand (**HL**) showed equally strong cytotoxic effect on HeLa, A549 and MDA-MB-453 cells as nickel complexes, which leads to conclusion that, considering interaction with these cell lines, cytotoxic properties are not enhanced upon complexation.

Examined nickel salt and salts of corresponding monodentates after 48h of incubation exhibited very low cytotoxic activity and did not reach IC<sub>50</sub> values in the range of applied concentrations (up to 100 µM) in all investigated cell lines.

## 2.8. Cell cycle analysis

Cell cycle analysis of HeLa cells treated with investigated complex **3**, appropriate ligand and cisplatin was performed by flow cytometry after staining with propidium iodide [19]. Cells were continually exposed to nickel complex, ligand and cisplatin for 24 and 48 h with increasing concentrations of agents ( $IC_{50}$  and  $1.5 \times IC_{50}$ ).

After 24h of continual treatment, there were no significant effects of nickel complex and ligand on cell cycle progression (**Fig. 4**). Examination of the histograms showing cell cycle phase distributions after 48h of incubation with investigated compounds indicated that both complex **3** and ligand induced perturbations of cell cycle of HeLa cells. Concentration dependent cell cycle arrest in the S phase, as well as decrease of percentage of cells in G1 phase, can be distinguished from untreated, control cell population. For both incubation times no significant increase of apoptotic fraction of cells (Sub-G1 fraction) was noted.

<**Fig. 4.**>

## 2.9. Apoptotic assay

Potential of the investigated nickel complex and corresponding ligand to induce apoptosis in HeLa cells compared to cisplatin was assessed by flow cytometry using Annexin V-FITC and PI dual staining. In **Fig. 5** representative dot plot diagrams are shown, with percentages of intact cells (Annexin V-FITC and PI negative), early apoptotic cells (Annexin V-FITC positive and PI negative), late apoptotic cells (Annexin V-FITC negative and PI positive) and necrotic cells (Annexin V-FITC negative and PI positive).

Data obtained from dot plot diagrams indicated that no significant increase in percentage of early and late apoptotic cells in treated cells compared to control was found. Moreover, there was no difference between apoptosis-inducing potential of lower and higher concentration of investigated agents, as well as between nickel complex and the ligand used in this study. These findings are consistent with the results of the tested compounds effect on cell cycle progression of HeLa cells. Opposite to cisplatin effect with clearly visible population of late apoptotic and

necrotic cells, mechanism of action of investigated agents remains unclear, with further investigations needed.

**<Fig. 5.>**

#### 2.10. DNA-binding activity and mode of DNA interaction

Non-covalent binding of small molecules with DNA occurs in three modes: intercalation binding, minor or major groove binding and electrostatic binding [20]. To deduce the binding mode of Ni(II) complex **3** and corresponding ligand **HL**, electronic absorption spectroscopy was performed. Electronic absorption spectra of nickel complex **3** recorded at different concentrations without or with fixed concentration of CT-DNA are shown in **Fig. 6a**. It was found that the spectra of **3** exhibit maximum absorption wavelength at 413 nm and after interaction with CT-DNA the formation of a **3**-CT-DNA was occurred. Hypochromism of about 34% observed with lower concentrations of compound indicates intercalation as the probable interaction. With increase of concentration of complex, hyperchromism (of about -14%) occurred as the result of possible non/covalent or electrostatic interactions between Ni(II) complex (**3**). The percentages were determined from  $(\varepsilon_{\text{DNA}} + \varepsilon_Q) - \varepsilon_B / (\varepsilon_{\text{DNA}} + \varepsilon_Q) \times 100$ , where  $\varepsilon_{\text{DNA}}$  is the extinction coefficient of CT-DNA,  $\varepsilon_Q$  is the extinction coefficient of free complex **3** and  $\varepsilon_B$  is the extinction coefficient of the bound **3**). The interaction of ligand **HL** with CT-DNA was monitored by UV-Vis spectroscopy in the same experimental conditions, **Fig. 6b**. In the spectrum of **HL** an increase of absorption intensity at 324 nm has also been observed after its interaction with CT-DNA with an increase of concentration of complex. This hyperchromism was calculated as -18% with red shift of 10 nm. These changes are typical of complexes bound to double stranded DNA through non-covalent interaction [21].

In order to obtain information on affinity of the complex **3** and ligand **HL** for CT-DNA, spectroscopic titration was performed. Absorbance of the solution of the complex with increasing concentration of CT-DNA (**Fig. 6c,d**) was measured at 255 nm. The binding constant  $K_B$  was determined using the equation 1 [22]:

$$[\text{DNA}] \times (\varepsilon_A - \varepsilon_F)^{-1} = [\text{DNA}] \times (\varepsilon_B - \varepsilon_F)^{-1} + K_B^{-1} \times (\varepsilon_B - \varepsilon_F)^{-1} \quad (1)$$

where  $\varepsilon_A$ ,  $\varepsilon_F$ ,  $\varepsilon_B$  are absorbance/[compound], extinction coefficient of the free compound and the extinction coefficient of the bound compound, respectively. The intrinsic binding constant  $K_B$  (**Fig. 6c** and **Fig. 6d**) of **3**-CT-DNA and **HL**-CT-DNA were  $3.22 \times 10^5 \text{ M}^{-1}$  and  $2.79 \times 10^5 \text{ M}^{-1}$ , respectively. The values are higher than the values of  $K_B$  described for classical intercalator, for example, ethidium-DNA [23] and smaller to those of DNA minor groove binders [24].

### <**Fig. 6.**>

To provide additional insight into the interactions between the complex **3**, ligand **HL** and CT-DNA, the experiments with the minor groove binder Hoechst 33258 [25] were performed. Hoechst 33258 (H) binds strongly and selectively with high affinity to double-stranded B-DNA structure and like other minor groove binders, it recognizes at least four AT base pairs. It binds by combination of hydrogen bonding, van der Waals contacts with the walls of the minor groove, and electrostatic interactions between its cationic structure and the DNA [26]. **Fig. 7a** shows the characteristic changes in fluorescence emission spectra of Hoechst 33258 after binding to DNA i.e. significant increase in the fluorescence intensity of H-CT-DNA (dark cyan curve in **Fig. 7a**) compared to free Hoechst. As shown in **Fig. 7b**, the addition of the **3** to CT-DNA caused appreciable reduction in the fluorescence intensity of H-CT-DNA complex in a concentration dependent way. The result was consistent with quenching curve shown in **Fig. 7c** that was applied to determine  $K$  by linear regression of a plot of  $I_0/I$  against  $r$ . The obtained fluorescence quenching data were analyzed according to the Stern-Volmer equation [27]:

$$I_0/I = 1 + Kr \quad (2)$$

where  $I_0$  and  $I$  represent the fluorescence intensities of EB-CT-DNA in absence and presence of the **3**, respectively,  $K$  is a Stern-Volmer quenching constant dependent on the ratio of the bound concentration of H to the bound concentration of DNA;  $r = [\mathbf{3}]/[\text{DNA}]$  is the ratio of the concentration of complex **3** to that of CT-DNA. The quenching plot demonstrated the quenching of H bound to CT-DNA by the complex **3** is in agreement with the linear Stern-Volmer Eq. (2)

with the correlation coefficients  $0.49 \pm 0.06$  and the corresponding quenching constant of H-CT-DNA system **3** was calculated as  $K = 2.82 \pm 0.28$ .

**<Fig. 7.>**

As shown previously, the solutions of Ni(II) complex **3** did not have fluorescence neither influenced on fluorescence of H (**Fig. 7a**, black and blue curves denoted as **3+H** and **3**, respectively). At contrast, ligand **HL** exhibited a fluorescence (in **Fig. 7d**, black curve denoted as **HL**). The enhancement of fluorescence upon binding of **HL** to CT-DNA was observed, (**Fig. 7d**, red curve). When both fluorophores were present in reaction mixture with CT-DNA (**Fig. 7d**, blue curve), the enhancement of fluorescence upon binding to nucleic acid was exceeded more than 6-fold at  $\lambda_{max}=486.4$  nm compared to H-CT-DNA system. The increasing in fluorescence intensity with the increase of concentration of **HL** showed in **Fig. 7e**.

The obtained results demonstrated that the ligand **HL** bind to DNA with different mode of interaction than groove binder Hoechst 33258 and complex of Ni(II).

### 2.11. DNA cleavage

The abilities of complex **3** and ligand **HL** to cleave double-stranded plasmid DNA were investigated using an agarose gel electrophoretic assay. The assay allows assessment of DNA strand cleavage by measuring the conversion of untreated supercoiled form (FI) plasmid DNA into the nicked form (FII) and linear form (FIII). As it shown in **Fig. 8** (lane 1), plasmid pUC19 consisted mainly of FI and FII. Upon the addition of complex **3** to the plasmid, the supercoiled DNA converted into nicked forms FII, the generation of the nicked form increased gradually up to  $30 \mu\text{M}$  of **3** (lane 4), when the bands of the supercoiled and linear forms almost disappeared and up to  $40 \mu\text{M}$  when no more DNA in running gel. The formation of possible multimer form was observed, with very slow mobility (stayed in the start of running). In order to determine the precise damaging effect of **3**, the smaller range of concentrations between  $20$  and  $30 \mu\text{M}$  was performed, **Fig. 8b**. The result showed the potential of complex **3** to nick one strand of the helix

producing relaxed circles like, the bacterial enzyme topoisomerase I. In the presence of all investigated concentrations of the ligand there were no observed changes of plasmid DNA forms.

**<Fig. 8.>**

### 3. Conclusion

In all synthesized square-planar nickel(II) complexes 2-(diphenylphosphino) benzaldehyde 4-phenylsemicarbazone was coordinated in deprotonated form via phosphorus, imine nitrogen and carbonyl oxygen atoms, while the fourth coordination place was occupied by one of three different monodentate ligands coordinated via nitrogen atom: cyanate, thiocyanate and azide, respectively. Investigated complexes exhibited moderate activity on Gram-positive bacteria, while only the azido complex showed moderate antibacterial activity on Gram-negative bacteria. The maximum activity against *C. albicans* was observed for ligand. On the basis of the obtained results it can be seen that biological activity of investigated complexes depends on the nature of monodentate ligands. All complexes **1–3** showed moderate activity to all tumor cell lines. The most pronounced cytotoxic activity (in the range of cisplatin) to HeLa cell line was observed for ligand and all the complexes. Similar cytotoxic activity of ligand and Ni(II) complexes on HeLa, A549 and MDA-MB-453 indicates that all cytotoxic properties were not changed upon complexation. Azido complex and ligand induced concentration dependent cell cycle arrest in the S phase, as well as decrease of percentage of cells in G1 phase, without significant increase of apoptotic fraction of cells.

The interaction of the complex **3** and ligand **HL** with CT-DNA results in changes in UV-Vis spectra typical for non-covalent bonding. The observed intrinsic binding constant of **3**-CT-DNA ( $3.22 \times 10^5 \text{M}^{-1}$ ) and **HL**-CT-DNA ( $2.79 \times 10^5 \text{M}^{-1}$ ) are higher than the values of  $K_B$  described for classical intercalator and smaller to those of DNA minor groove binders. Additional experiments with the minor groove binder Hoechst 33258 demonstrated that the ligand **HL** bind to DNA on different mode of interaction than groove binder Hoechst 33258 and complex **3**. The results of DNA cleavage experiments showed that complex **3** possessed activity similar to enzyme topoisomerase I. Having in mind the results of cytotoxicity experiment, cell cycle analysis and DNA spectroscopic and electrophoretic studies the mechanism of action for

complex **3** is DNA damaging. Comparison with the previously described Ni(II) complexes with condensation derivative of 2-(diphenylphosphino)benzaldehyde and ethyl carbazate [11] suggests that small structural changes of tridentate phosphine ligand results in significant differences in biological activity as a consequence of liphophilicity and stability of complexes.

#### 4. Experimental

##### 4.1. Material and methods

2-(Diphenylphosphino)benzaldehyde (97%) and 4-phenylsemicarbazide (97%) were obtained from Aldrich. The ligand was obtained by condensation reaction of 2-(diphenylphosphino)benzaldehyde and 4-phenylsemicarbazide using a previously described method [12]. IR spectra were recorded on a Perkin–Elmer FT-IR 1725X spectrometer using the ATR technique in the region 4000–400 cm<sup>-1</sup>. <sup>1</sup>H NMR (500 MHz), <sup>13</sup>C NMR (125 MHz) and 2D NMR spectra were recorded on a Bruker Avance 500 spectrometer in CDCl<sub>3</sub> at room temperature using TMS as internal standard for <sup>1</sup>H and <sup>13</sup>C. Chemical shifts are expressed in ppm ( $\delta$ ) values and coupling constants ( $J$ ) in Hz. Elemental analyses (C, H, and N) were performed by standard micro-methods using the ELEMENTARVario ELIII C.H.N.S.O analyzer.

##### 4.2. Synthesis of [NiLOCN] (**1**)

A mixture of 0.06 g (0.18 mmol) Ni(BF<sub>4</sub>)<sub>2</sub>·6H<sub>2</sub>O and 0.07 g (0.17 mmol) of **HL** ligand was dissolved in 50 mL ethanol and then 0.05 g (0.8 mmol) NaOCN was added. The mixture was refluxed for 2 h. The reaction solution was left to stand at room temperature while the reddish crystals arose from the solution. Yield 0.06 g (68 %) IR (vs-very strong, s-strong, m-medium, w-weak): 3578 (w), 3325 (m), 3056 (w), 2251 (vs), 1600 (m), 1565 (m), 1537 (s), 1503 (s), 1438 (s), 1359 (s), 1240 (m), 1091 (m), 1021 (m), 904 (w), 824 (w), 747 (m), 690 (m). Elemental analysis calcd for C<sub>27</sub>H<sub>21</sub>N<sub>4</sub>O<sub>2</sub>PNi: N 10.71 %, C 61.99 %, H 4.05 %, found: N 10.64 %, C 61.96 %, H 3.98 %.

##### 4.3. Synthesis of [NiLSCN] (**2**)

In the mixture of 0.05 g (0.20 mmol)  $\text{Ni}(\text{AcO})_2 \cdot 4\text{H}_2\text{O}$  and 0.07 g (0.17 mmol) of **HL** ligand in 40 mL ethanol 0.04 g (0.5 mmol)  $\text{NH}_4\text{NCS}$  was added. The mixture was refluxed for 2 h. The reaction solution was left to stand at room temperature while the dark reddish crystals arose from the solution. Yield 0.06g (67 %) IR (vs-very strong, s-strong, m-medium, w-weak): 3335 (m), 3055 (w), 2107 (s), 2023 (w), 1595 (m), 1600 (m), 1533 (s), 1499 (s), 1436 (s), 1368 (m), 1354 (m), 1231 (w), 1093 (w), 1016 (w), 913 (w), 848 (w), 822 (w), 750 (m), 689 (m), 615 (w). Elemental analysis calcd for  $\text{C}_{27}\text{H}_{21}\text{N}_4\text{OPSNi}$ : N 10.39 %, C 60.14 %, H 3.93 %, S 5.95 %, found: N 10.36 %, C 60.18 %, H 3.98 %, S 5.83 %.

#### 4.4. *Synthesis of $[\text{NiLN}_3]$ (**3**)*

A mixture of 0.07 g (0.20 mmol)  $\text{Ni}(\text{BF}_4)_2 \cdot 6\text{H}_2\text{O}$  and 0.08 g (0.19 mmol) of ligand was dissolved in 50 mL methanol and then 0.10 g (1.5 mmol)  $\text{NaN}_3$  was added. The mixture was refluxed for 2 h. The reddish crystals arose from the reaction solution at room temperature. Yield 0.07 g (70 %) IR (vs-very strong, s-strong, m-medium, w-weak): 3255 (w), 3066 (w), 2034 (vs), 1600 (w), 1562 (w), 1539 (m), 1491 (s), 1439 (vs), 1357 (s), 1078 (w), 1019 (w), 755 (m), 708 (m), 695 (m). Elemental analysis calcd for  $\text{C}_{26}\text{H}_{21}\text{N}_6\text{OPNi}$ : N 16.21 %, C 58.61 %, H 4.06 %, found: N 16.06 %, C 58.64 %, H 4.06 %.

#### 4.5. *X-ray structure determinations*

Crystal data and refinement parameters of compounds **1–3** are listed in Table 7. The X-ray intensity data were collected at 150 K with Agilent SuperNova dual source with an Atlas detector equipped with mirror-monochromated Cu  $\text{K}\alpha$  radiation ( $\lambda = 1.54184 \text{ \AA}$ ). The data were processed using CRYSTALIS PRO [28]. The structures were solved by direct methods (SIR-92 [29]) and refined by a full-matrix least-squares procedure based on  $F^2$  using SHELXL-97 [30]. All non-hydrogen atoms were refined anisotropically. The N1 and C8 bonded hydrogen atoms were located in a difference map and refined with the distance restraints (DFIX) with N-H = 0.88 and C-H = 1.00 and with  $U_{\text{iso}}(\text{H}) = 1.2U_{\text{eq}}(\text{N})$  or  $U_{\text{iso}}(\text{H}) = 1.2U_{\text{eq}}(\text{C})$ , respectively. All other

hydrogen atoms were included in the model at geometrically calculated positions and refined using a riding model. Compound **2** crystallize in the noncentrosymmetric space group *Pn* with the value of the Flack parameter 0.01(2).

CCDC 995551–995553 contains the supplementary crystallographic data for **1**, **2**, and **3**, respectively. These data can be obtained free of charge from The Cambridge Crystallographic Data Centre via [www.ccdc.cam.ac.uk/data\\_request/cif](http://www.ccdc.cam.ac.uk/data_request/cif).

#### <Table 7>

#### 4.6. Computational details

All calculations have been performed using the Amsterdam Density Functional (ADF) program package [31] version 2013.01., with general gradient approximation consisting of OPTX [32] for the exchange and PBE [33] functional for correlation (OPBE [34]). Molecular orbitals were expanded in an uncontracted set of Slater type orbitals (STOs) [35], of triple- $\zeta$  quality containing diffuse functions plus one set of polarization functions (TZP [36]). Default integration and gradient convergence criterions were used. Analytical harmonic frequencies [37] were calculated in order to ascertain that the optimized structures correspond to the minima on the potential energy surface. In order to check the possible influence of an environment, we also performed additional calculations with a dielectric continuum model (COSMO [38]) (using water as a solvent) as implemented in ADF [39].

#### 4.7. Antimicrobial activity

The antimicrobial activity of the ligand and three Ni(II) complexes was investigated on eight different laboratory control strains of bacteria, i.e., the Gram-positive: *Staphylococcus aureus* (ATCC 25923), *Staphylococcus epidermidis* (ATCC 12228), *Kocuria rhizophila* (ATCC 9341), *Bacillus subtilis* (ATCC 6633) and the Gram-negative: *Escherichia coli* (ATCC 10536), *Klebsiella pneumoniae* (NCIMB 9111), *Pseudomonas aeruginosa* (ATCC 9027), *Salmonella abony* (NCTC 6017) and one strain of yeast, i.e., *Candida albicans* (ATCC 10231). All tests were performed in Müller Hinton broth for the bacterial strains and in

Sabouraud dextrose broth for the yeast. Overnight broth cultures of each strain were prepared, and the final concentration in each well was adjusted to  $2 \times 10^6$  CFU/mL for the bacteria and  $2 \times 10^5$  CFU/mL for the yeast. The tested substances were dissolved in 1% dimethyl sulfoxide (DMSO) and then diluted to the highest concentration. Twofold serial concentrations of the compounds were prepared in a 96-well microtiter plate over the concentration range 62.5–1000 µg/mL. The microbial growth was determined after 24 h incubation at 37 °C for the bacteria and after 48 h incubation at 26 °C for the fungi. The MIC is defined as the lowest concentration of compound at which no visible growth of microorganism is observed.

#### 4.8. Cell culture

Human cervix carcinoma cells (HeLa), melanoma cells (FemX), lung adenocarcinoma cells (A549), colon cancer cells (LS-174), breast cancer cells (MDA-MB-453) and human foetal lung fibroblast cells (MRC-5) cells were maintained as monolayer culture in the Roswell Park Memorial Institute (RPMI) 1640 nutrient medium (Sigma Chemicals Co, USA). Human myelogenous leukaemia cells (K562) were maintained in suspension culture. RPMI 1640 nutrient medium was prepared in sterile ionized water, supplemented with penicillin (192 U/mL), streptomycin (200 mg/mL), 4-(2-hydroxyethyl) piperazine-1-ethanesulfonic acid (HEPES) (25 mM), L-glutamine (3 mM) and 10% of heat-inactivated foetal calf serum (FCS) (pH 7.2). The cells were grown at 37 °C in 5% CO<sub>2</sub> and humidified air atmosphere, by twice weekly subculture.

#### 4.9. MTT assay

Cytotoxicity of the investigated nickel complexes (**1–3**), the appropriate ligand (**HL**), nickel salt and salts of corresponding monodentates in comparison to cisplatin, was determined using the 3-(4,5-dimethylthiazol-2yl)-2,5-diphenyltetrazolium bromide (MTT, Sigma-Aldrich) assay [40]. Cells were seeded in 96-well cell culture plates (NUNC): HeLa (4000 c/w), FemX (4000 c/w), A549 (6000 c/w), LS-174 (7000 c/w), MDA-MB-453 (4000 c/w) and MRC-5 (5000 c/w) in culture medium and grown for 24 h. K562 (5000 c/w) cells were seeded 2 h before

treatment. Stock solutions of investigated agents were made in DMSO at concentration of 10 mM, and afterwards diluted with nutrient medium to desired final concentrations (in range up to 100  $\mu$ M). Cisplatin (CDDP) stock solution was made in 0.9% NaCl at concentration of 1.66 mM and afterwards diluted with nutrient medium to desired final concentrations (in range up to 100  $\mu$ M). The final concentration of DMSO per well did not exceed 1%. Solutions of various concentrations of examined compounds were added to the wells, except the control wells where only nutrient medium was added. All samples were done in triplicate. Nutrient medium with corresponding agent concentrations but without target cells was used as a blank, also in triplicate.

Cells were incubated for 48 h with the test compounds at 37 °C, with 5% CO<sub>2</sub> in humidified atmosphere. After incubation, 20  $\mu$ L of MTT solution, 5 mg/mL in phosphate buffer solution (PBS), pH 7.2, was added to each well. Samples were incubated for 4 h at 37 °C with 5% CO<sub>2</sub> in humidified atmosphere. Formazan crystals were dissolved in 100  $\mu$ L 10% sodium dodecyl sulfate (SDS). Absorbance was recorded on the ThermoLabsystems 408 Multiskan EX 200–240 V after 24 h at a wavelength of 570 nm. Concentration IC<sub>50</sub> ( $\mu$ M) was defined as the concentration of drug producing 50% inhibition of cell survival. It is determined from the cell survival diagrams.

#### 4.10. Cell cycle analysis

Flow-cytometric analysis of cell cycle phase distribution of HeLa cells, treated with investigated nickel complex (**3**), corresponding ligand (**HL**) and cisplatin as reference compound, was performed after staining fixed HeLa cells with propidium iodide (PI) [40]. HeLa cells were seeded at density of  $2 \times 10^5$  cells/well at 6-well plate (NUNC) and grown in nutrition medium. After 24 h cells were continually exposed to investigated complexes with concentrations that correspond to IC<sub>50</sub> and 1.5×IC<sub>50</sub> (determined for 48 h treatment). After 24 and 48 h of continual treatment, cells were collected by trypsinization, washed twice with ice-cold PBS, and fixed for 30 min in 70% EtOH. After fixation, cells were washed again with PBS, and incubated with RNaseA (1 mg/mL) for 30 min at 37 °C. Cells were than stained with PI (400 mg/mL) 15 min before flow-cytometric analysis. Cell cycle phase distribution were

analysed using a fluorescence activated sorting cells (FASC) Calibur Becton Dickinson flow cytometer and Cell Quest computer software.

#### *4.11. Apoptotic assay*

Induction of apoptosis by nickel complex (**3**), corresponding ligand (**HL**) and cisplatin as positive control in HeLa cells was evaluated by Annexin V–FITC apoptosis detection kit (BD Biosciences Cat. No. 65874x, Pharmingen San Diego, CA, USA). Briefly,  $1 \times 10^6$  HeLa cells/mL were treated with IC<sub>50</sub> and  $1.5 \times IC_{50}$  concentrations of nickel complex (**3**), ligand (**HL**) and cisplatin for 48 h. After treatment cells were washed twice with cold PBS and then resuspended in 200  $\mu$ L binding buffer (10 mM HEPES/NaOH pH 7.4, 140 mM NaCl, 2.5 mM CaCl<sub>2</sub>). 100  $\mu$ L of the solution ( $1 \times 10^5$  cells) was transferred to a 5 mL culture tube and 5  $\mu$ L of Annexin V–FITC and 5  $\mu$ L of PI were added. Cells were gently vortexed and incubated for 15 min at 25 °C in the dark. After that, 400  $\mu$ L of binding buffer was added to each tube and then analysed using a FACS Calibur Becton Dickinson flow cytometer and Cell Quest Pro computer software.

#### *4.12. Spectroscopic studies*

For an UV-Vis measurement, to DNA solution (10  $\mu$ L of CT-DNA stock solution) was added a small volume of a concentrated solution of complex **3** and ligand **HL** (final concentration 300  $\mu$ M) and the volume was adjusted up 1 mL with 40 mM bicarbonate buffer pH 8.4. Reaction mixtures were incubated at 37 °C during 60 min with occasional vortexing. Spectra of CT-DNA of the same concentrations were also recorded. UV-Vis spectra were recorded in a UV Cintra 40 UV/Visible spectrometer operating from 200 to 800 nm in 1.0 cm quartz cells.

The control was DNA–Hoechst 33258 solution. The competitive interactions of **3** and **HL** and fluorescence probe Hoechst 33258 (28  $\mu$ M at final concentration) with CT-DNA were performed. Reaction mixtures containing 98.56  $\mu$ M of CT-DNA (calculated per phosphate) and different concentrations of the compound in 1 mL of 40 mM bicarbonate solution (pH 8.4) were

incubated for 60 min with occasional vortexing. 1.5  $\mu$ L of 1% Hoechst was added to each solution, and the incubation was prolonged for the next 15 min and the mixture was analyzed by fluorescence measurement. The control was CT-DNA–Hoechst 33258 solution. For fluorescence titrations different amounts of CT-DNA were added to 0.04 mM solution of **3**. Fluorescence spectra were collected using a Thermo Scientific Lumina Fluorescence spectrometer (Finland) equipped with a 150 W Xenon lamp. The slits on the excitation and emission beams were fixed at 10 nm. All measurements were performed by excitation at 350 nm in the range of 390 nm to 650 nm. The details are given in Figure legends.

#### 4.13. DNA cleavage assay

Double-stranded closed circular high copy plasmid pUC19 (2686 base pairs with a molecular weight of  $1.74 \times 10^6$  Da, isolated from *E. coli*) was purchased from Fermentas Life Sciences (EU). 0.5  $\mu$ g of pUC19 in a 20  $\mu$ L reaction mixtures in bicarbonate buffer (40 mM sodium bicarbonate, pH 8.4), were incubated with different concentrations of the nickel complex **3** or ligand **HL** at 37 °C for 60 min. The control sample was prepared with 3  $\mu$ L of DMSO instead of the complex. The reaction mixtures were vortexed from time to time. The reaction was terminated by short centrifugation at 10000 rpm and adding 7  $\mu$ L of loading buffer (0.25 % bromophenol blue, 0.25 % xylene cyanol FF and 30 % glycerol in TAE buffer, pH 8.24 (40 mM Tris-acetate, 1 mM EDTA). The samples were subjected to electrophoresis on 0.8 % agarose gel (Amersham Pharmacia-Biotech, Inc) prepared in TAE buffer pH 8.24. The electrophoresis was performed at a constant voltage (80 V) for 35 min (until bromophenol blue had passed through 75 % of the gel). After electrophoresis, the gel was stained for 20 min by soaking it in an aqueous ethidium bromide solution (0.5  $\mu$ g/mL), and after that was visualized under UV light.

#### Acknowledgments

This work was supported by the Ministry of Education, Science and Technological development of the Republic of Serbia (Grant OI 172055 and Grant III 41026). We thank the

Slovenian Research Agency (ARRS) through program P-0175 for financial support and EN-FIST Centre of Excellence, Dunajska 156, 1000 Ljubljana, Slovenia, for using SuperNova diffractometer.

#### **Appendix A. Supplementary data**

Supplementary data related to this article can be found at...

## References

- [1] I. Ott, On the medicinal chemistry of gold complexes as anticancer drugs, *Coord. Chem. Rev.* 253 (2009) 1670–1681.
- [2] M.J. McKeage, L. Maharaj, S.J. Berners-Price, Mechanisms of cytotoxicity and antitumor activity of gold(I) phosphine complexes: the possible role of mitochondria, *Coord. Chem. Rev.* 232 (2002) 127–135.
- [3] R. Galassi, A. Burini, S. Ricci, M. Pellei, M. Rigobello, A. Citta, A. Dolmella, V. Gandin, C. Marzano, Synthesis and characterization of azolate gold(I) phosphane complexes as thioredoxin reductase inhibiting antitumor agents, *Dalton Trans.* 41 (2012) 5307–5318.
- [4] W.M. Motswainyana, M.O. Onani, A.M. Madiehe, M. Saibu, N. Thovhogi, R.A. Lalancette, Imino-phosphine palladium(II) and platinum(II) complexes: Synthesis, molecular structures and evaluation as antitumor agents, *J. Inorg. Biochem.* 129 (2013) 112–118.
- [5] M.M. Dorđević, D.A. Jeremić, M.V. Rodić, V.S. Simić, I.D. Brčeski, V.M. Leovac, Synthesis, structure and biological activities of Pd(II) and Pt(II) complexes with 2-(diphenylphosphino)benzaldehyde 1-adamantoylhydrazone, *Polyhedron* 68 (2014) 234–240.
- [6] S. Rollas, Ş.G. Küçükgüzel, Biological Activities of Hydrazone Derivatives, *Molecules* 12 (2007) 1910–1939.
- [7] V. Radulović, A. Bacchi, G. Pelizzi, D. Sladić, I. Brčeski, K. Andđelković, Synthesis, structure, and antimicrobial activity of complexes of Pt(II), Pd(II), and Ni(II) with the condensation product of 2-(diphenylphosphino)benzaldehyde and semioxamazide, *Monatsh. Chem.* 137 (2006) 681–691.
- [8] N. Malešević, T. Srđić, S. Radulović, D. Sladić, V. Radulović, I. Brčeski, K. Andđelković, Synthesis and characterization of a novel Pd(II) complex with the condensation product of 2-(diphenylphosphino)benzaldehyde and ethyl hydrazinoacetate. Cytotoxic activity of the synthesized complex and related Pd(II) and Pt(II) complexes, *J. Inorg. Biochem.* 100 (2006) 1811–1818.

- [9] M. Milenković, A. Bacchi, G. Cantoni, S. Radulović, N. Gligorijević, S. Aranđelović, D. Sladić, M. Vučić, D. Mitić, K. Andelković, Synthesis, characterization and biological activity of Co(III) complex with the condensation product of 2-(diphenylphosphino)benzaldehyde and ethyl carbazole, Inorg. Chim. Acta 395 (2013) 33–43.
- [10] M. Milenković, G. Cantoni, A. Bacchi, V. Spasojević, M. Milenković, D. Sladić, N. Krstić, K. Andelković, Synthesis, characterization and antimicrobial activity of Pd(II) and Fe(III) complexes with ethyl (2E)-2-[2-(diphenylphosphino)benzylidene]hydrazinecarboxylate, Polyhedron, <http://dx.doi.org/10.1016/j.poly.2014.01.022>.
- [11] M. Milenković, A. Bacchi, G. Cantoni, J. Vilipić, D. Sladić, M. Vučić, N. Gligorijević, K. Jovanović, S. Radulović, K. Andelković, Synthesis, characterization and biological activity of three square-planar complexes of Ni(II) with ethyl (2E)-2-[2-(diphenylphosphino)benzylidene]hydrazinecarboxylate and monodentate pseudohalides, Eur. J. Med. Chem. 68 (2013) 111–120.
- [12] A. Barandov, U. Abram, Chloro-2-(diphenylphosphino)benzaldehyde 4-phenyl semicarbazone-P, N, N')methoxooxorhenium(V) – a Semicarbazone Complex with an Unusual Coordination Mode, Z. Anorg. Allg. Chem. 633 (2007) 1897–1899.
- [13] S.B. Novaković, G.A. Bogdanović, I.D. Brčeski, V.M. Leovac, Different intermolecular interactions in azido[2-(diphenylphosphino)-benzaldehyde semicarbazone  $\kappa^2 P,N^1,O$ ]nickel(II), Acta Crystallogr. C, 65 (2009) m263–m265.
- [14] G. Bogdanović, A. Spasojević-de Biré, B. Prelesnik, V. Leovac, Transition Metal Complexes with Thiosemicarbazide-Based Ligands. 33. [4-(2-Diphenylphosphino- $\alpha$ -ethoxybenzyl-P)-3-methyl-1-salicylideneisothiosemicarbazido- $N^1$ ,  $N^4$ ,  $O$ ]nickel(II), Acta Crystallogr. C, 54 (1998) 766–768.
- [15] S. Güveli, T. Bal-Demirci, N. Özdemir, B. Ülküseven, Nickel(II) complexes of ONS and ONN chelating thiosemicarbazones with triphenylphosphine co-ligands, Transit. Metal Chem. 34 (2009) 383–388.

- [16] J.C. Wasilke, G. Wu, X. Bu, G. Kehr, G. Erker, Ruthenium Carbene Complexes Featuring a Tridentate Pincer-type Ligand, *Organometallics*, 24 (2005) 4289–4297.
- [17] S. Durran, M.R.J. Elsegood, S.R. Hammond, M.B. Smith, Flexible  $\kappa^4$ -PNN'O-tetradeятate ligands: synthesis, complexation and structural studies, *Dalton Trans.* 39 (2010) 7136–7146.
- [18] K. Brandenburg, DIAMOND, Crystal and Molecular Structure Visualization Version 3.2, Crystal Impact GbR, Bonn, Germany.
- [19] R. Supino, Methods in Molecular Biology, in: S. O'Hare, C.K. Atterwill (Eds.), *In vitro Toxicity Testing Protocols*, Humana Press, New Jersey, 1995, 137–149.
- [20] I. Turel, J. Kljun, Interactions of metal ions with DNA, its constituents and derivatives, which may be relevant for anticancer research, *Curr. Top. Med. Chem.* 11 (2011) 2661–2687.
- [21] T. Hirohama, Y. Kuranuki, E. Ebina, T. Sugizaki, H. Arii, M. Chikira, P.T. Selvi, M. Palaniandavar, Copper(II) complexes of 1,10-phenanthroline-derived ligands: Studies on DNA binding properties and nuclease activity, *J. Inorg. Biochem.* 99 (2005) 1205–1215.
- [22] R. Vijayalakshmi, M. Kanthimathi, V. Subramanian, B.U. Nair, DNA Cleavage by a Chromium(III) Complex, *Biochem. Biophys. Res. Commun.* 271 (2000) 731–734.
- [23] M.J. Waring, Complex formation between ethidium bromide and nucleic acids, *J. Mol. Biol.* 13 (1965) 269–274.
- [24] D.L. Ma, C.M. Che, F M. Siu, M. Yang, K.Y. Wong, DNA binding and cytotoxicity of ruthenium(II) and rhenium(I) complexes of 2-amino-4-phenylamino-6-(2-pyridyl)-1,3,5-triazine, *Inorg. Chem.* 46 (2007) 740–749.
- [25] D. Suh, J.B. Chaires, Criteria for the mode of binding of DNA binding agents, *Bioorgan. Med. Chem.* 3 (1995) 723–728.
- [26] R. Kakkar, R. Garg, Suruchi, Towards understanding the molecular recognition process in Hoechst–DNA complexes *J. Mol. Struct.* 584 (2002) 37–44.

- [27] N.C. Garbett, N.B. Hammond, D.E. Graves, Influence of the Amino Substituents in the Interaction of Ethidium Bromide with DNA, *Biophys. J.* 87 (2004) 3974–3981.
- [28] Oxford Diffraction, CrysAlis PRO, Oxford Diffraction Ltd., Yarnton, England, 2009.
- [29] A. Altomare, G. Cascarano, C. Giacovazzo, A. Guagliardi, Completion and Refinement of Crystal Structures with SIR92, *J. Appl. Crystallogr.* 26 (1993) 343–350.
- [30] G.M. Sheldrick, A short history of SHELX, *Acta Crystallogr. A*, 64 (2008) 112–122.
- [31] (a) E.J. Baerends, T. Ziegler, J. Autschbach, D. Bashford, A. Bérces, F.M. Bickelhaupt, C. Bo, P.M. Boerrigter, L. Cavallo, D.P. Chong, L. Deng, R.M. Dickson, D.E. Ellis, M. van Faassen, L. Fan, T.H. Fischer, C.F. Guerra, M. Franchini, A. Ghysels, A. Giammona, S.J.A. van Gisbergen, A.W. Götz, J.A. Groeneveld, O.V. Gritsenko, M. Grüning, S. Gusarov, F.E. Harris, P. van den Hoek, C.R. Jacob, H. Jacobsen, L. Jensen, J.W. Kaminski, G. van Kessel, F. Kootstra, A. Kovalenko, M.V. Krykunov, E. van Lenthe, D.A. McCormack, A. Michalak, M. Mitoraj, S.M. Morton, J. Neugebauer, V.P. Nicu, L. Noddleman, V.P. Osinga, S. Patchkovskii, M. Pavanello, P.H.T. Philipsen, D. Post, C.C. Pye, W. Ravenek, J.I. Rodríguez, P. Ros, P.R.T. Schipper, G. Schreckenbach, J.S. Seldenthuis, M. Seth, J.G. Snijders, M. Solà, M. Swart, D. Swerhone, G. te Velde, P. Vernooijs, L. Versluis, L. Visscher, O. Visser, F. Wang, T.A. Wesolowski, E.M. van Wezenbeek, G. Wiesenecker, S.K. Wolff, T.K. Woo, A.L. Yakovlev, ADF2013, SCM, Theoretical Chemistry, Vrije Universiteit, Amsterdam, The Netherlands, <http://www.scm.com> (b) C.F. Guerra, J.G. Snijders, G. teVelde, E. Baerends, *Theor. Chem. Acc.* 99 (1998) 391–403; (c) G. te Velde, F.M. Bickelhaupt, E.J. Baerends, C.F. Guerra, S.J.A. van Gisbergen, J.G. Snijders, T. Ziegler, *J. Comput. Chem.* 22 (2001) 931–967.
- [32] N.C. Handy, A. Cohen, *Molec. Phys.* 99 (2001) 403–412.
- [33] J.P. Perdew, K. Burke, M. Ernzerhof, *Phys. Rev. Lett.* 77 (1996) 3865–3868.
- [34] M. Swart, A. W. Ehlers, K. Lammertsma, *Molec. Phys.* 102 (2004) 2467–2474.
- [35] E. van Lenthe, E.J. Baerends, *J. Comput. Chem.* 24 (2003) 1142–1156.
- [36] E. van Lenthe, A. Ehlers, E.-J. Baerends, *J. Chem. Phys.* 110 (1999) 8943–8953.

- [37] (a) A. Bérçes, R.M. Dickson, L. Fan, H. Jacobsen, D. Swerhone, T. Ziegler, *Comput. Phys. Commun.* 100 (1997) 247–262; (b) H. Jacobsen, A. Bérçes, D. Swerhone, T. Ziegler, *Comput. Phys. Commun.* 100 (1997) 263–276.
- [38] (a) A. Klamt, G. Schüürmann, *J. Chem. Soc. Perkin Trans. 2* (1993) 799–805; (b) A. Klamt, *J. Phys. Chem.* 99 (1995) 2224–2235; (c) A. Klamt, V. Jones, *J. Chem. Phys.* 105 (1996) 9972–9981.
- [39] (a) C.C. Pye, T. Ziegler, *Theor. Chem. Acc.* 101 (1999) 396–408; (b) M. Swart, E. Rösler, F. M. Bickelhaupt, *Eur. J. Inorg. Chem.* (2007) 3646–3654.
- [40] M.G. Ormerod, Analysis of DNA-general methods, in: M.G. Ormerod (Ed.), *Flow Cytometry, a Practical Approach*, Oxford University Press, New York, 1994, pp. 119–125.

*Scheme captions*

**Scheme 1.** Complexes of Ni(II) with 2-(diphenylphosphino)benzaldehyde 4-phenyl semicarbazone

**Figure captions**

**Fig. 1.** ORTEP plot of **1** from the X-ray crystal structure with thermal ellipsoids at 50% probability for non-H atoms and open circles for H-atoms.

**Fig. 2.** ORTEP plot of **2** from the X-ray crystal structure with thermal ellipsoids at 50% probability for non-H atoms and open circles for H-atoms.

**Fig. 3.** ORTEP plot of **3** from the X-ray crystal structure with thermal ellipsoids at 50% probability for non-H atoms and open circles for H-atoms.

**Fig. 4.** Effect of the Ni(II) complex (**3**), corresponding ligand (**HL**) and cisplatin (**CDDP**) on cell cycle progression of HeLa cells following 24 and 48 h incubation with concentrations of investigated complexes corresponding to IC<sub>50</sub> and 1.5×IC<sub>50</sub>. Controls were untreated cells (incubated with nutrient medium only). Histograms presented are representative of three independent experiments

**Fig. 5.** Dot plot diagrams obtained by flow-cytometric analysis of treated HeLa cells after dual staining with Annexin V-FITC and PI. Annexin V-FITC/PI staining was performed after 48 hours of HeLa cells exposure to nickel complex (**3**), ligand (**HL**) and CDDP at concentrations corresponding to IC<sub>50</sub> and 1.5×IC<sub>50</sub>. Representative dot plots of three independent experiments are given, presenting intact cells at lower-left quadrant, FITC(-)/PI(-); early apoptotic cells at lower-right quadrant, FITC(+)/PI(-); late apoptotic or necrotic cells at upper-right quadrant, FITC(+)/PI(+); and necrotic cells at upper-left quadrant, FITC(-)/PI(+).

**Fig. 6.** Absorption spectra of: (a) **3** (10 µM, 20 µM, 30 µM and 40 µM) without CT-DNA and with CT-DNA (98 µM); (b) **HL** (10 µM, 20 µM, 30 µM and 40 µM) without CT-DNA and with CT-DNA (98 µM); (c) **3** (40 µM) without CT-DNA and with CT-DNA (9.85 µM, 19.7 µM, 29.6 µM, 39.4 µM, 49.3 µM, 59.1 µM, 69 µM, 78.8 µM, 88.7 µM and 98 µM); (d) **HL** (40 µM) without CT-DNA and with CT-DNA (9.85 µM, 19.7 µM, 29.6 µM, 39.4 µM, 49.3 µM, 59.1 µM, 69 µM, 78.8 µM, 88.7 µM and 98 µM). The arrows show the changes in absorbance upon increasing amounts of CT-DNA. Insets: plot of [DNA]/(ε<sub>A</sub>–ε<sub>F</sub>) versus [DNA] (M).

**Fig. 7.** Fluorescence spectra of Hoechst 33258 (H) bound to CT-DNA (98  $\mu$ M) in absence and presence of (a) **3** at concentrations of 10  $\mu$ M, 20  $\mu$ M, 30  $\mu$ M and 40  $\mu$ M (curves from top to bottom); and (d) **HL** (40  $\mu$ M); changes of fluorescence intensities at  $\lambda_{max} = 444$  nm and at  $\lambda_{max} = 486.4$  nm with concentration of **3** (b) and **HL** (e), respectively; and (c) quenching curve of H bound to CT-DNA at  $\lambda_{max} = 444$  nm system by complex **3**;  $r = [3]/[CT\text{-DNA}]$ .

**Fig. 8.** Agarose electrophoresis of plasmid pUC19 DNA (13nM) without (lane 1) and pUC19 (13 nM) with (a): **3** (10  $\mu$ M, 20  $\mu$ M, 30  $\mu$ M and 40  $\mu$ M, lanes 2, 3, 4 and 5, respectively) and **HL** (10  $\mu$ M, 20  $\mu$ M and 40  $\mu$ M, lanes 6, 7 and 8); (b) **3** (20  $\mu$ M, 22.5  $\mu$ M, 25  $\mu$ M, 27.5  $\mu$ M and 30  $\mu$ M). The arrows denote the mobilities of the slowest nicked forms FII.

**Table 1**Selected bond lengths ( $\text{\AA}$ ) and angles ( $^\circ$ ) of compounds **1**, **2** and **3**.

	<b>1</b>	<b>2</b>	<b>3</b>
Ni1–P1	2.1397(4)	2.1366(12)	2.1409(7)
Ni1–O1	1.8861(10)	1.878(3)	1.8770(17)
Ni1–N3	1.8613(13)	1.866(4)	1.882(2)
Ni1–N4	1.8443(15)	1.846(4)	1.873(2)
N1–C7	1.3681(19)	1.376(6)	1.364(3)
N2–N3	1.3908(16)	1.397(5)	1.405(3)
N2–C7	1.326(2)	1.317(6)	1.328(3)
N3–C8	1.296(2)	1.290(6)	1.284(3)
N4–C27	1.166(2)	1.158(6)	-
O1–C7	1.2767(19)	1.287(5)	1.290(3)
O2–C27	1.200(2)	-	--
S1–C27	-	1.613(5)	
N4–N5	-	-	1.213(3)
N5–N6	-	-	1.148(3)
P1–Ni1–O1	172.14(4)	168.92(11)	165.25(6)
P1–Ni1–N3	95.01(4)	93.23(12)	94.79(6)
P1–Ni1–N4	90.01(4)	92.74(13)	89.22(8)
N3–Ni1–N4	174.88(6)	174.02(18)	173.62(10)
N3–N2–C7	108.60(12)	108.4(3)	108.36(18)
Ni1–O1–C7	108.90(9)	108.5(3)	109.07(15)
N4–C27–O2	179.01(17)	-	-
N4–C27–S1	-	178.9(5)	-
N4–N5–N6	-	-	174.6(3)

**Table 2**Hydrogen bonding geometry for **1**, **2** and **3**.

D – H … A	<i>d</i> (D – H)/ Å	<i>d</i> (H … A)/ Å	<i>d</i> (D … A)/ Å	$\angle$ (DHA)/ °	Symmetry transformation for acceptors
<b>1</b> N1-H1N…O2	0.858(15)	2.133(16)	2.9672(19)	164.1(18)	-x+1, y+1/2, -z+1/2
<b>2</b> N1-H1N…S1	0.88(2)	2.67(4)	3.371(4)	137(4)	x+1/2, -y, z+1/2
<b>3</b> N1-H1N…N2	0.879(17)	2.278(18)	3.150(3)	172(3)	-x+2, -y, -z+1

**Table 3**<sup>1</sup>H NMR spectral data of **HL**, **1**, **2** and **3**.

Assignment	Chemical shift (ppm), multiplicity, number of H-atoms, coupling constant <i>J</i> (Hz)			
	<b>HL</b>	<b>1</b>	<b>2</b>	<b>3</b>
C1	8.56 (d, 1H, <i>J</i> =5.0 Hz)	7.93 (s, 1H)	7.90 (s, 1H)	7.94 (s, 1H)
C3	6.80 (dd, 1H, <i>J</i> =10.0 Hz, <i>J</i> =5.0 Hz)	7.25 (m, 1H)	7.25 (m, 1H)	7.23 (m, 1H)
C4	7.34 (t, 1H, <i>J</i> =5.0 Hz)	7.34 (m, 1H)	7.35 (m, 1H)	7.33 (t, 1H, <i>J</i> =7.5 Hz)
C5	7.47 (t, 1H, <i>J</i> =5.0 Hz)	7.60 (m, 1H)	7.61 (m, 1H)	7.56 (m, 1H)
C6	8.23 (dd, 1H, <i>J</i> =10.0 Hz, <i>J</i> =5.0 Hz)	7.42 (m, 1H)	7.38 (m, 1H)	7.38 (m, 1H)
C9	7.22 (m, 4H)	7.79 (m, 4H)	7.78 (m, 4H)	7.75 (m, 4H)
C10	7.41 (m, 4H)	7.52 (m, 4H)	7.56 (m, 4H)	7.50 (m, 4H)
C11	7.41 (m, 2H)	7.60 (m, 2H)	7.61 (m, 2H)	7.60 (m, 2H)
C13	7.58 (dd, 2H, <i>J</i> =7.5 Hz, <i>J</i> =5.0 Hz)	7.37 (m, 2H)	7.35 (m, 2H)	7.43 (dd, 2H, <i>J</i> =10.0 Hz, <i>J</i> =1.0 Hz)
C14	7.28 (t, 2H, <i>J</i> =7.5 Hz)	7.25 (m, 2H)	7.25 (m, 2H)	7.23 (m, 2H)
C15	7.01 (tt, 1H, <i>J</i> =10.0 Hz, <i>J</i> =5.0 Hz)	6.97 (t, 1H, <i>J</i> =5.0 Hz)	6.97 (t, 1H, <i>J</i> =5.0 Hz)	6.96 (tt, 1H, <i>J</i> =7.5 Hz, <i>J</i> =1.0 Hz)
NH2	8.79 (s, 1H)	6.76 (s, 1H)	7.03 (s, 1H)	6.38 (s, 1H)
NH1	10.84 (s, 1H)			

**Table 4**<sup>13</sup>C NMR spectral data of **HL**, **1**, **2** and **3**.

Assignment	<sup>13</sup> C NMR chemical shift (ppm), coupling constant, <i>J</i> (Hz)			
	<b>HL</b>	<b>1</b>	<b>2</b>	<b>3</b>
C1	138.9 (d, <i>J</i> =7.5 Hz)	147.7	147.8	147.4
C2	135.8 (d, <i>J</i> =10.0 Hz)	136.6 (d, <i>J</i> =18.8 Hz)	136.2 (d, <i>J</i> =10.0 Hz)	136.9 (d, <i>J</i> =17.9 Hz)
C3	133.0	134.0	133.8	134.1
C4	129.4	130.4 (d, <i>J</i> =6.2 Hz)	130.6	130.0 (d, <i>J</i> =6.5 Hz)
C5	129.2	132.9	133.1	132.7
C6	127.1	133.8 (d, <i>J</i> =10.0 Hz)	133.9	133.7
C7	135.2 (d, <i>J</i> =18.8 Hz)	118.3 (d, <i>J</i> =45.0 Hz)	117.4 (d, <i>J</i> =53.7 Hz)	118.4 (d, <i>J</i> =44.6 Hz)
C8	137.8 (d, <i>J</i> =18.8 Hz)	126.7 (d, <i>J</i> =57.5 Hz)	126.1 (d, <i>J</i> =56.2 Hz)	126.7 (d, <i>J</i> =55.0 Hz)
C9	133.5 (d, <i>J</i> =20.0 Hz)	133.5 (d, <i>J</i> =10.0 Hz)	133.5	133.6 (d, <i>J</i> =10.6 Hz)
C10	128.8	129.4 (d, <i>J</i> =11.2 Hz)	129.5	129.2 (d, <i>J</i> =11.1 Hz)
C11	128.9	132.1 (d, <i>J</i> =2.5 Hz)	132.2	131.8 (d, <i>J</i> =2.3 Hz)
C12	139.1	139.0	138.8	139.1
C13	119.7	118.9	118.8	118.7
C14	128.5	128.9	128.9	128.9
C15	122.5	122.5	122.6	122.4
C16	152.8	168.8	168.9	168.8
C(OCN)		136.5		
C(SCN)			143.3	

**Table 5**

The antimicrobial activity of ligand **HL** and Ni(II) complexes (MIC values in mM).

Microorganism	<b>HL</b>	<b>1</b>	<b>2</b>	<b>3</b>	Cefotaxime	Amphotericin B
<i>Staphylococcus aureus</i> ATCC 25923	1.181	0.956	0.464	0.956	0.027	not tested
<i>Staphylococcus epidermidis</i> ATCC 12228	1.181	0.478	0.464	0.478	0.007	not tested
<i>Kocuria rhizophila</i> ATCC 9341	1.181	0.478	0.464	0.478	0.055	not tested
<i>Bacillus subtilis</i> ATCC 6633	1.181	0.956	0.927	0.478	0.027	not tested
<i>Escherichia coli</i> ATCC 10536	1.181	0.956	0.927	0.478	0.014	not tested
<i>Klebsiella pneumoniae</i> NCIMB 9111	1.181	0.956	0.927	0.239	0.007	not tested
<i>Pseudomonas aeruginosa</i> ATCC 9027	1.181	0.956	1.854	0.239	0.027	not tested
<i>Salmonella abony</i> NCTC 6017	0.590	0.956	0.464	0.239	0.055	not tested
<i>Candida albicans</i> ATCC 10231	0.295	0.956	0.464	0.478	not tested	0.007

**Table 6**

Results of MTT assay presented as IC<sub>50</sub> ( $\mu$ M) values obtained after 48 h treatment. IC<sub>50</sub> values are calculated as mean values obtained from two to three independent experiments and presented with their standard deviations.

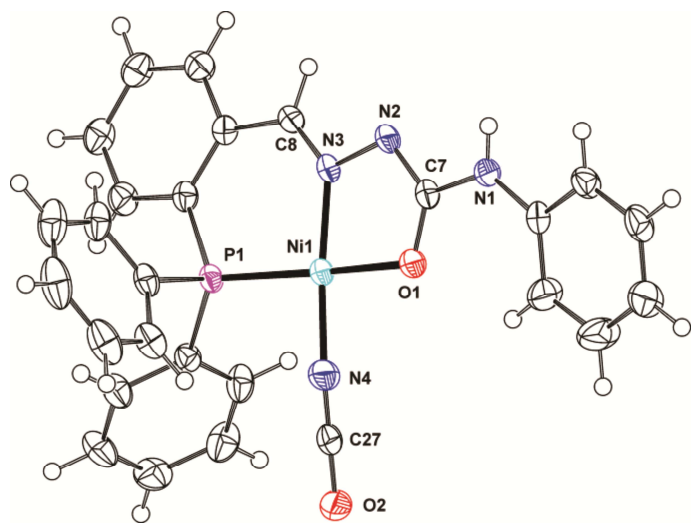
	<b>HeLa</b>	<b>K562</b>	<b>A549</b>	<b>FemX</b>	<b>MDA-MB-453</b>	<b>LS-174</b>	<b>MRC-5</b>
<b>1</b>	8.10 $\pm$ 3.69	42.79 $\pm$ 17.44	19.22 $\pm$ 5.68	32.10 $\pm$ 14.39	31.41 $\pm$ 4.39	66.08 $\pm$ 13.29	6.52 $\pm$ 0.93
<b>2</b>	9.33 $\pm$ 1.87	65.92 $\pm$ 3.03	19.04 $\pm$ 5.88	37.42 $\pm$ 10.90	34.52 $\pm$ 6.10	78.74 $\pm$ 11.06	7.07 $\pm$ 0.13
<b>3</b>	7.27 $\pm$ 1.80	29.66 $\pm$ 3.69	25.25 $\pm$ 1.63	27.50 $\pm$ 0.37	36.33 $\pm$ 10.85	65.11 $\pm$ 0.57	5.91 $\pm$ 1.51
<b>HL</b>	7.38 $\pm$ 2.95	> 100	26.12 $\pm$ 2.47	> 100	28.81 $\pm$ 8.61	> 100	11.21 $\pm$ 5.09
<b>NiCl<sub>2</sub>·6H<sub>2</sub>O</b>	> 100	> 100	> 100	> 100	> 100	> 100	> 100
<b>NH<sub>4</sub>SCN</b>	> 100	> 100	> 100	> 100	> 100	> 100	> 100
<b>NaOCN</b>	> 100	> 100	> 100	> 100	> 100	> 100	> 100
<b>NaN<sub>3</sub></b>	> 100	> 100	> 100	> 100	> 100	> 100	> 100
<b>CDDP</b>	7.79 $\pm$ 2.32	19.77 $\pm$ 0.89	17.20 $\pm$ 0.70	10.77 $\pm$ 0.88	3.75 $\pm$ 0.12	22.41 $\pm$ 7.18	30.26 $\pm$ 2.98

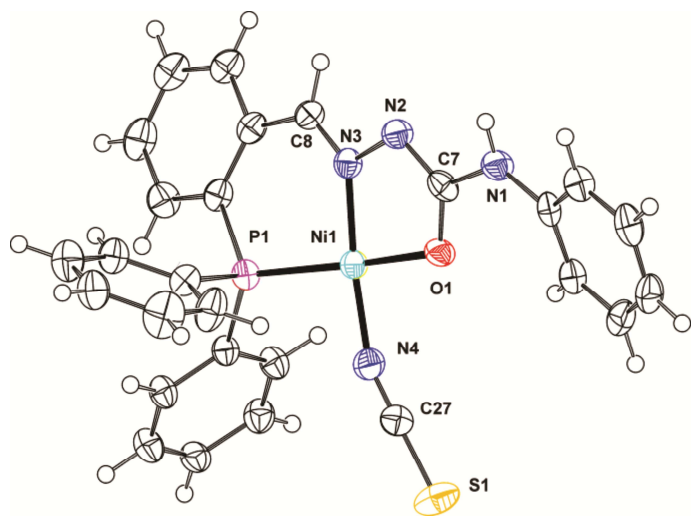
The sign (>) indicates that IC<sub>50</sub> value is not reached in the examined range of concentrations (the sign is in front of the maximum value of the concentration in the examined range of concentrations).

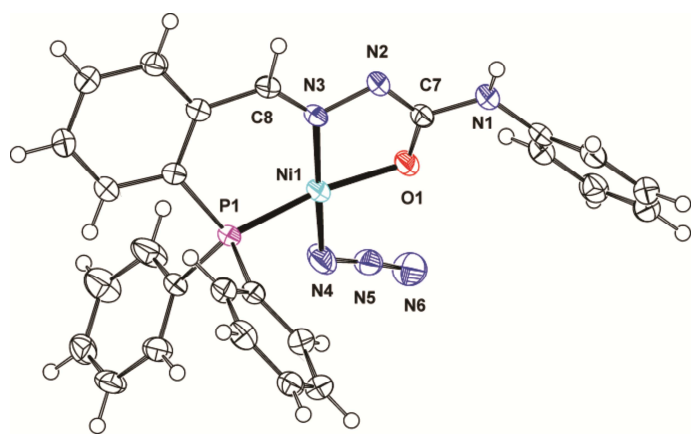
**Table 7**Crystal data and structure refinement details for **1**, **2** and **3**.

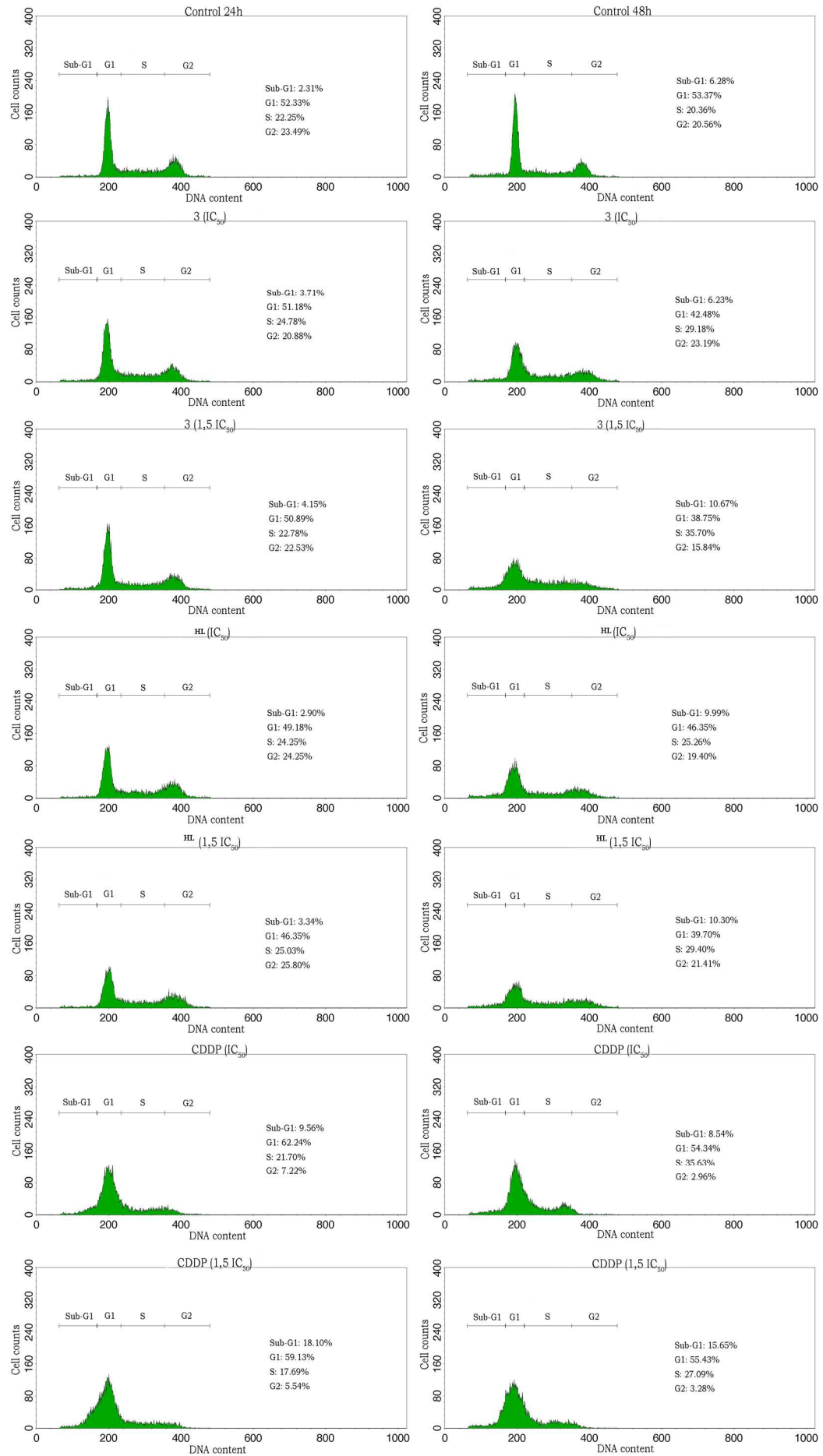
	<b>1</b>	<b>2</b>	<b>3</b>
formula	C <sub>27</sub> H <sub>21</sub> N <sub>4</sub> NiO <sub>2</sub> P	C <sub>27</sub> H <sub>21</sub> N <sub>4</sub> NiOPS	C <sub>26</sub> H <sub>21</sub> N <sub>6</sub> NiOP
Fw (g mol <sup>-1</sup> )	523.16	539.22	523.17
crystal size (mm)	0.35 × 0.02 × 0.02	0.30 × 0.20 × 0.15	0.40 × 0.15 × 0.05
crystal color	red	red	red
crystal system	monoclinic	monoclinic	triclinic
space group	P2 <sub>1</sub> /c	Pn	P-1
<i>a</i> (Å)	7.18840(10)	9.8241(4)	9.1467(8)
<i>b</i> (Å)	15.1949(2)	8.0651(3)	11.6862(9)
<i>c</i> (Å)	21.7013(2)	15.5431(8)	12.5247(7)
$\alpha$ (°)	90	90	70.736(7)
$\beta$ (°)	95.4390(10)	90.300(5)	68.842(7)
$\gamma$ (°)	90	90	75.028(7)
<i>V</i> (Å <sup>3</sup> )	2359.70(5)	1231.50(9)	1163.77(15)
<i>Z</i>	4	2	2
calcd density (g cm <sup>-3</sup> )	1.473	1.454	1.493
<i>F</i> (000)	1080	556	540
no. of collected reflns	15474	3262	11918
no. of independent reflns	4792	1950	4759
<i>R</i> <sub>int</sub>	0.0270	0.0294	0.0484
no. of reflns observed	4256	1900	4106
no. parameters	322	322	322
<i>R</i> [ <i>I</i> > 2σ ( <i>I</i> )] <sup>a</sup>	0.0293	0.0303	0.0468
<i>wR</i> <sub>2</sub> (all data) <sup>b</sup>	0.0785	0.0783	0.1413
<i>Goof</i> , <i>S</i> <sup>c</sup>	1.029	0.999	1.050
maximum/minimum residual electron density (e Å <sup>-3</sup> )	+0.22/-0.45	+0.22/-0.32	+0.45/-0.87

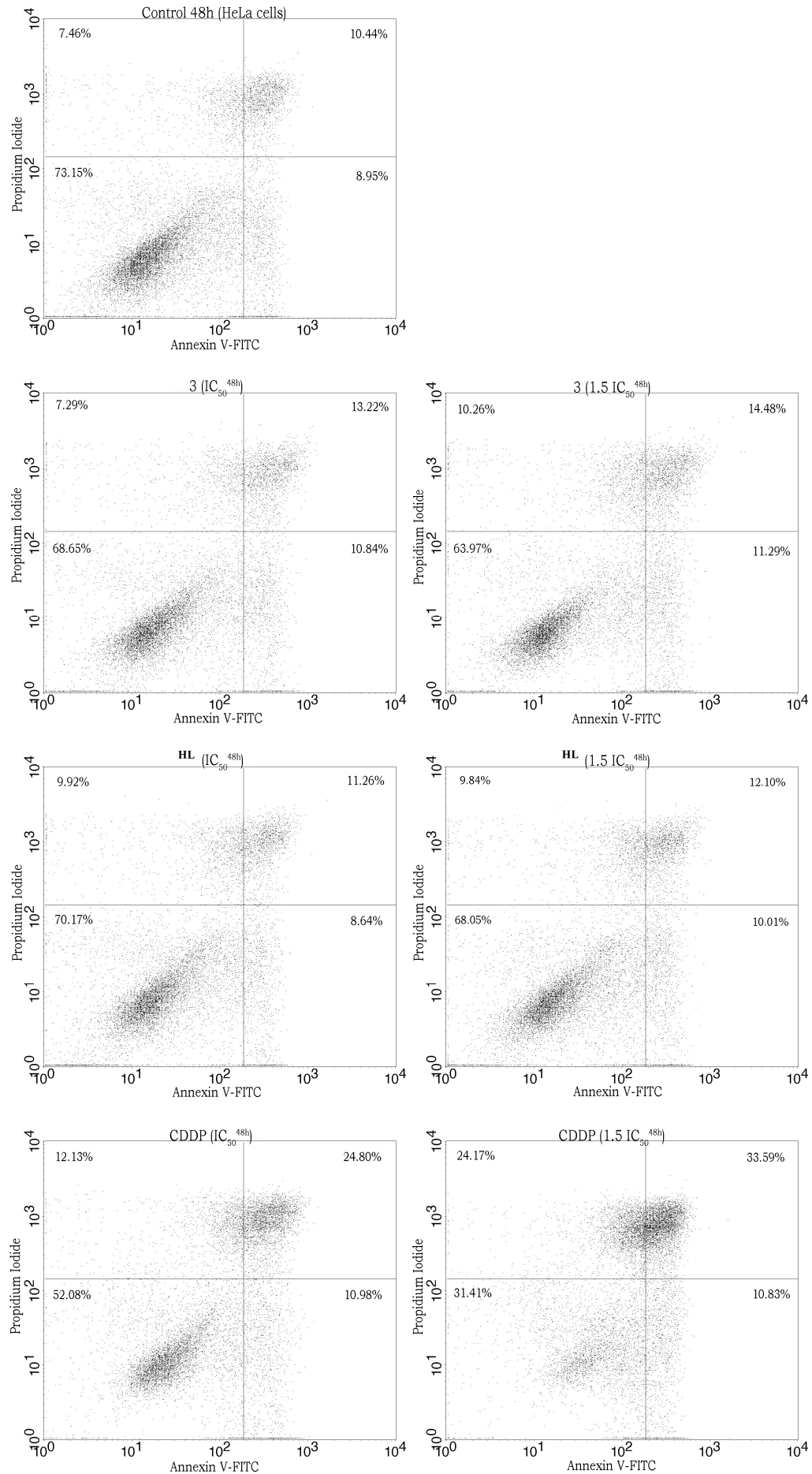
<sup>a</sup>  $R = \sum ||F_o| - |F_c|| / \sum F_o$ .<sup>b</sup>  $wR_2 = \{\sum [w(F_o^2 - F_c^2)^2] / \sum [w(F_o^2)^2]\}^{1/2}$ .<sup>c</sup>  $S = \{\sum [(F_o^2 - F_c^2)^2] / (n/p)\}^{1/2}$  where *n* is the number of reflections and *p* is the total

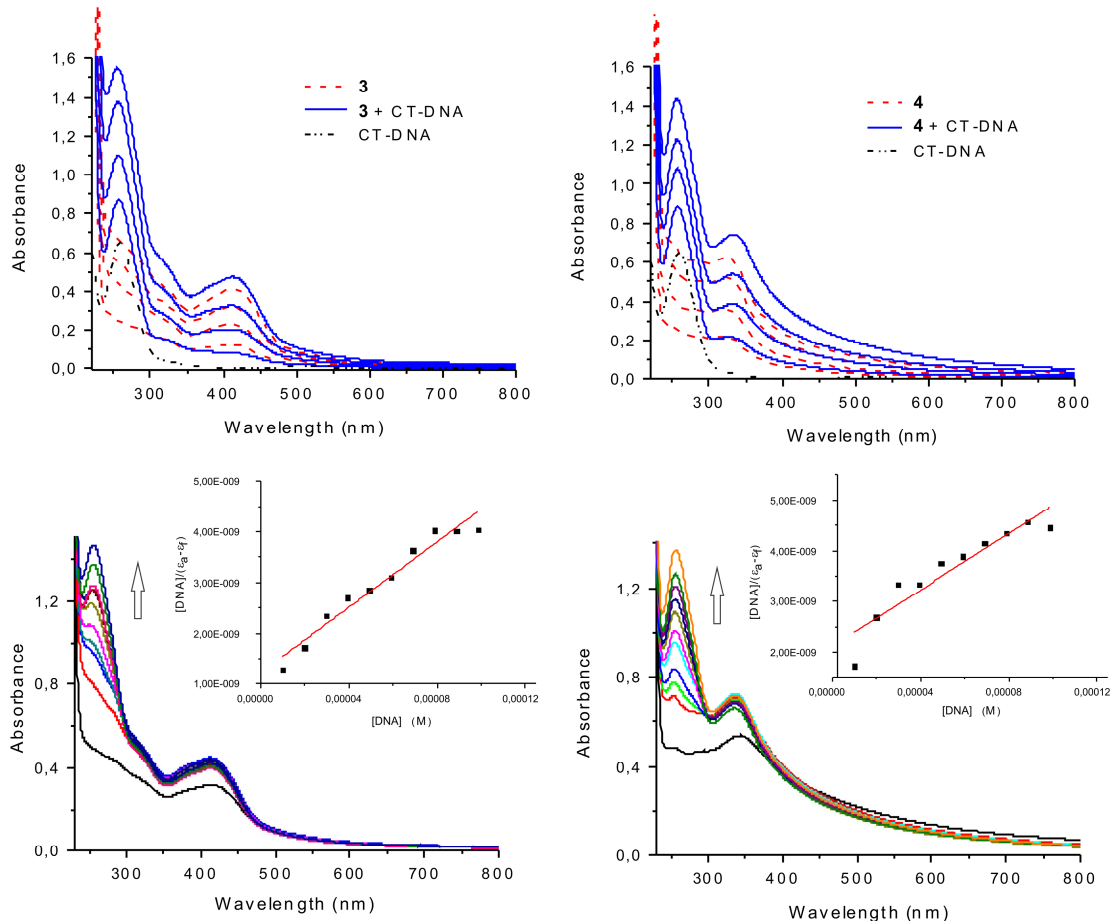




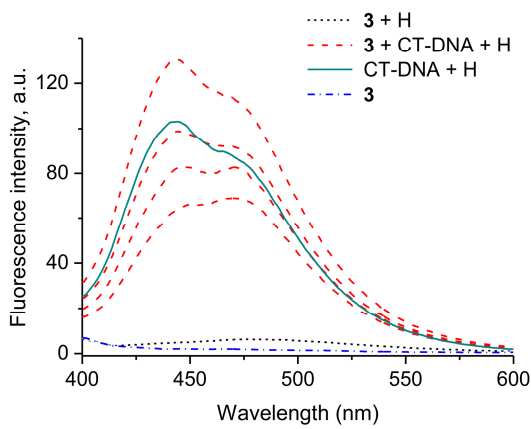




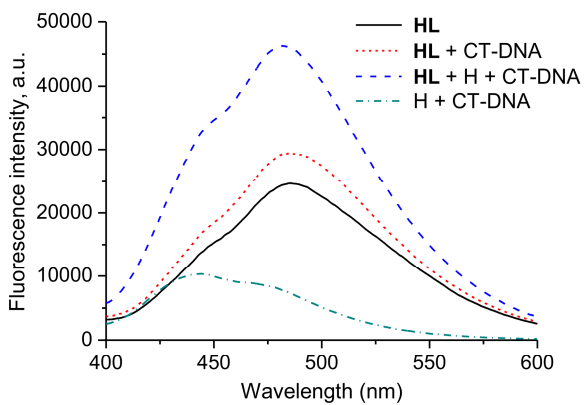




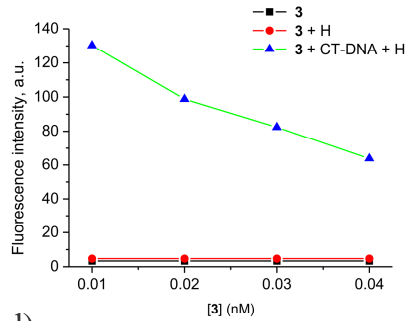
a)



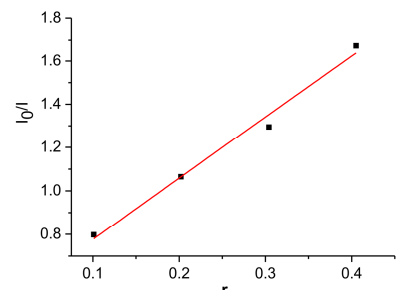
b)



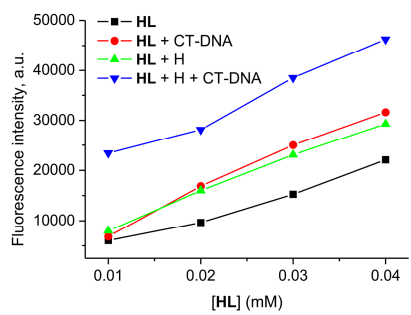
c)

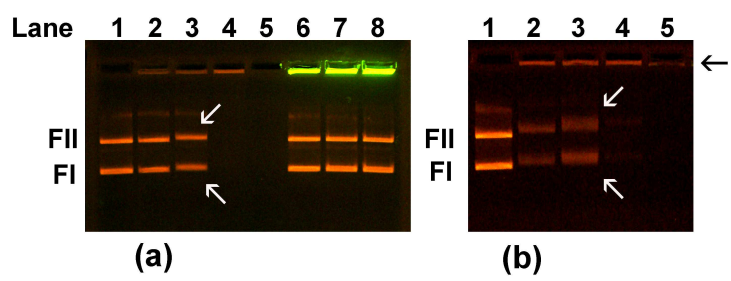


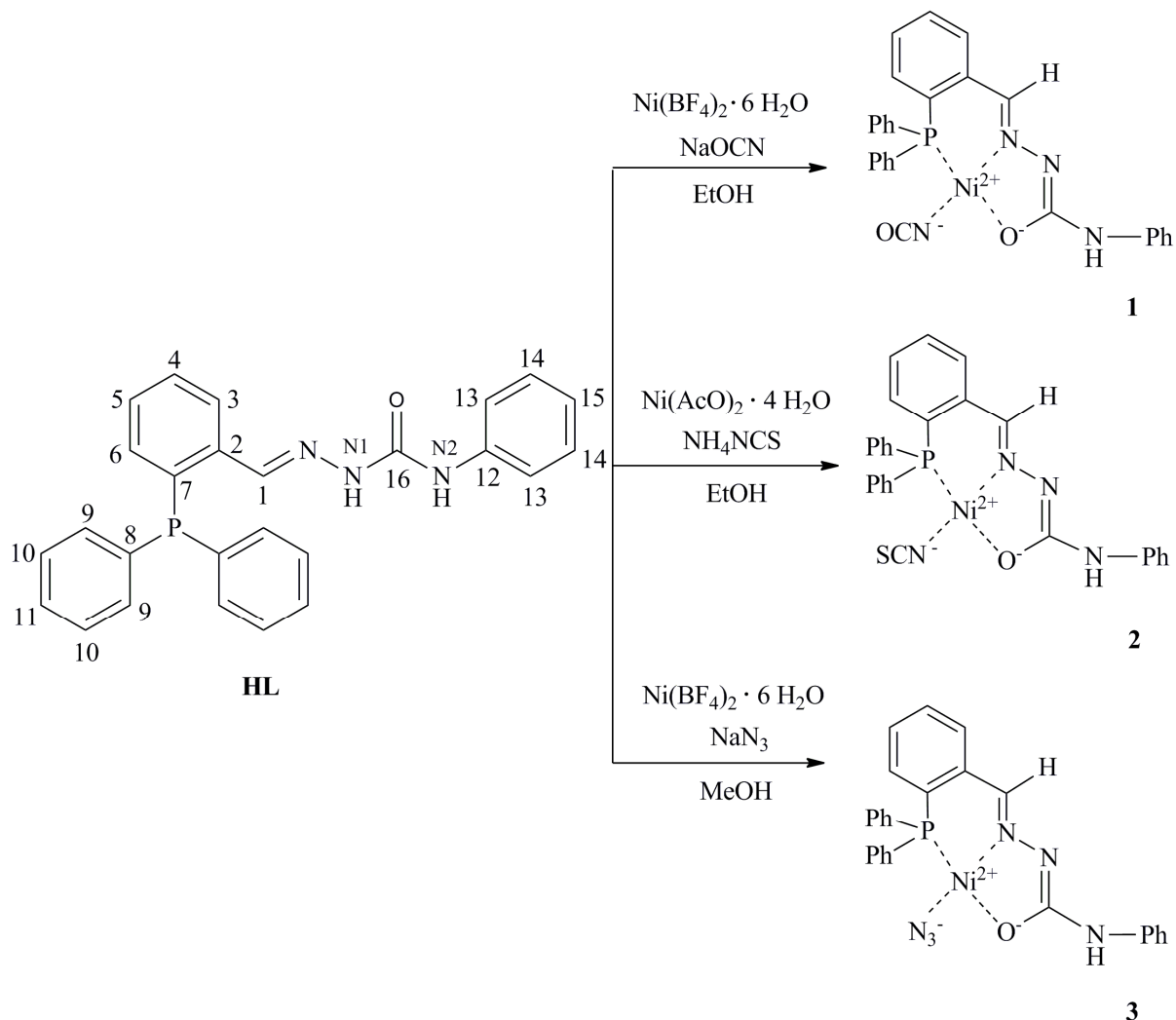
d)



e)







- Square-planar complexes of Ni(II) with PNO set of donor atoms
- Antimicrobial and cytotoxic activities
- Cytotoxic activity to HeLa cell lines in the range of cisplatin
- Effect on cell cycle progression in tumor cells

**Supplementary Material****Synthesis, characterization, DFT calculation and biological activity of square-planar Ni(II) complexes with tridentate PNO ligands and monodentate pseudohalides. Part II.**

Milica Milenković<sup>a</sup>, Andrej Pevec<sup>b</sup>, Iztok Turel<sup>b</sup>, Miroslava Vujčić<sup>c</sup>, Marina Milenković<sup>d</sup>, Katarina Jovanović<sup>e</sup>, Nevenka Gligorijević<sup>e</sup>, Siniša Radulović<sup>e</sup>, Marcel Swart<sup>f,g</sup>, Maja Gruden-Pavlović<sup>a</sup>, Kawther Adaila<sup>a</sup>, Božidar Čobeljić<sup>a</sup> and Katarina Andelković<sup>a<sup>1</sup></sup>

<sup>a</sup>*Faculty of Chemistry, University of Belgrade, Studentski trg 12–16, 11000 Belgrade, Serbia*

<sup>b</sup>*Faculty of Chemistry and Chemical Technology, University of Ljubljana, Aškerčeva 5, 1000 Ljubljana, Slovenia*

<sup>c</sup>*Institute of Chemistry, Technology and Metallurgy, University of Belgrade, Njegoševa 12, P.O. Box 815, 11000 Belgrade, Serbia*

<sup>b</sup>*Department of Microbiology and Immunology, Faculty of Pharmacy, University of Belgrade, Vojvode Stepe 450, Serbia*

<sup>e</sup>*Institute for Oncology and Radiology of Serbia, Department of Experimental Oncology, Laboratory for Experimental Pharmacology, Pasterova 14, Belgrade, Serbia*

<sup>f</sup>*Institució Catalana de Recerca i Estudis Avançats (ICREA), Pg. Lluís Companys 23, 08010 Barcelona, Spain*

<sup>g</sup>*Institut de Química Computacional i Catàlisi and Departament de Química, Universitat de Girona, Campus Montilivi, 17071 Girona, Spain*

---

<sup>1</sup> Corresponding author. Tel.: +381 11 3282 750.

E-mail address: kka@chem.bg.ac.rs (K. Andelković).

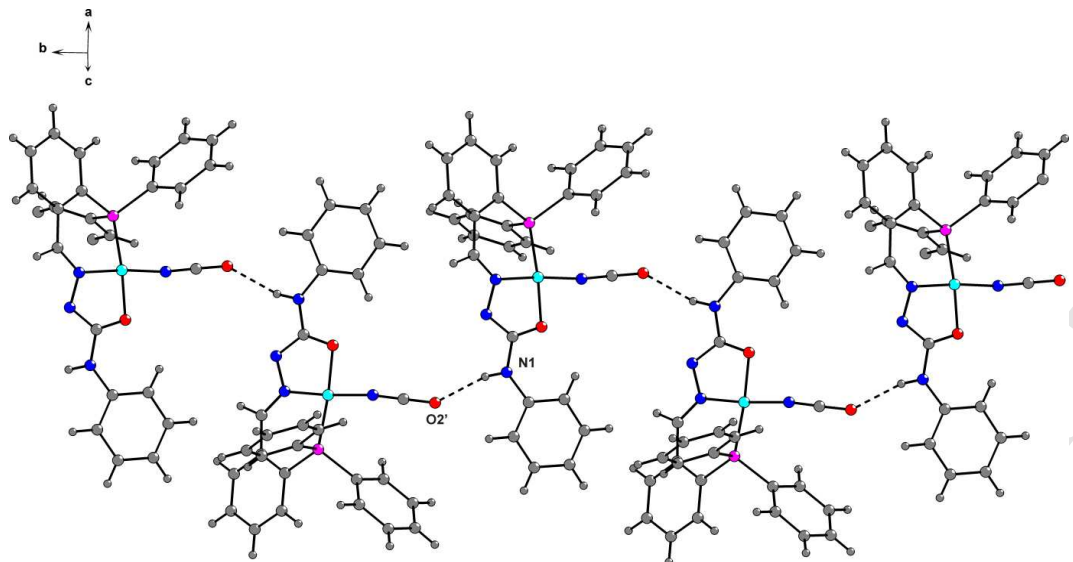


**Fig. S1.** DIAMOND [18] view of **1** showing the polymeric chain in the crystal structure [Symmetry code: (i)  $-x+1, y+1/2, -z+1/2$ ].

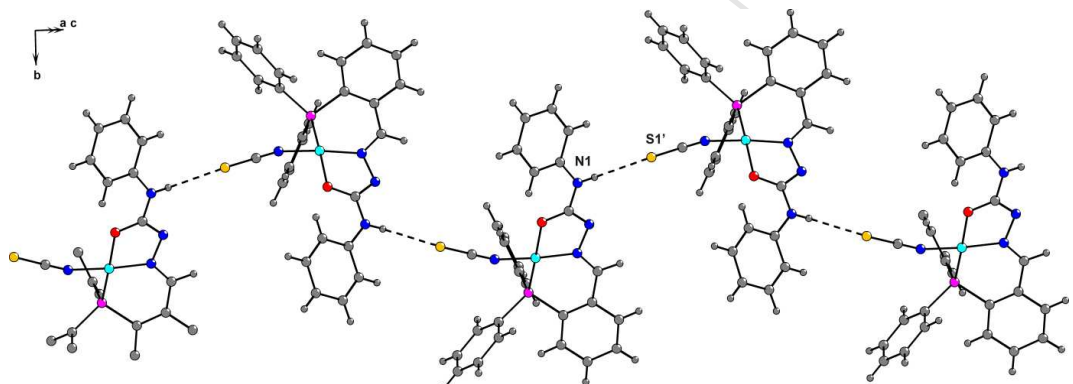


**Fig. S2.** DIAMOND [18] view of **2** showing the polymeric chain in the crystal structure [Symmetry code: (i)  $x+1/2, -y, z+1/2$ ].

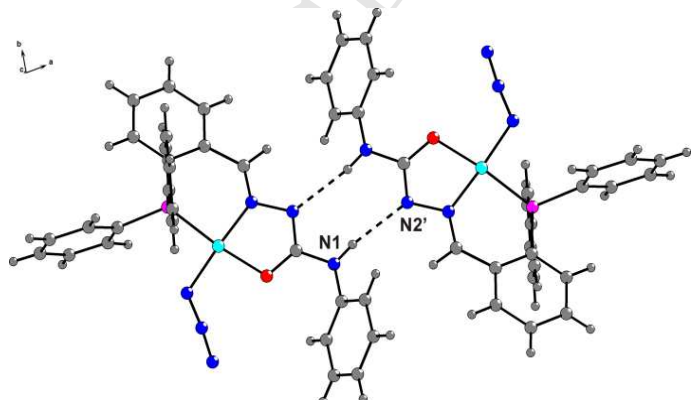


**Fig. S3.** DIAMOND [18] view of **3** showing the intermolecular N-H...N interactions in the crystal structure [Symmetry code: (i)  $-x+2, -y, -z+1$ ].

Energies and coordinates of Ni complexes:

NiL(NCS) : -8658.1310 kcal/mol

NiL(SCN) : -8653.8160 kcal/mol

$$\Delta E = -4.315 \text{ kcal/mol}$$

NiL (N<sub>3</sub>) : -8707.4624 kcal/mol

NiL(NCO) : -8731.3342 kcal/mol

NiL(OCN) : -8714.3121 kcal/mol

$$\Delta E = -17.0221 \text{ kcal/mol}$$

Coordinates:

		H	6.35950000	-2.15440000
			0.24900000	
NiL(NCS)		C	5.17680000	-0.41180000 -
Ni	0.45630000	0.18030000	-	0.16740000
0.05980000		H	4.24230000	-0.87750000
P	-1.64990000	0.11060000		0.13100000
0.20070000		C	5.18230000	0.91910000 -
S	0.58670000	-4.17740000		0.62180000
1.48360000		C	2.72360000	1.42660000 -
O	2.35570000	0.22640000	-	0.51830000
0.20090000		C	-0.34380000	2.88100000 -
N	4.04050000	1.72600000	-	0.79930000
0.71690000		H	0.03380000	3.87260000 -
N	1.86870000	2.43790000	-	1.05880000
0.68230000		C	-1.77500000	2.71290000 -
N	0.57560000	1.97700000	-	0.85730000
0.55980000		C	-2.50230000	3.82610000 -
N	0.52190000	-1.56940000		1.34000000
0.43940000		H	-1.95840000	4.74130000 -
C	6.40190000	1.51020000	-	1.57420000
1.00610000		C	-3.87680000	3.76100000 -
H	6.40370000	2.54330000	-	1.53960000
1.35870000		H	-4.40920000	4.63280000 -
C	7.59030000	0.78750000	-	1.91850000
0.93780000		C	-4.56780000	2.57320000 -
H	8.52270000	1.26430000	-	1.27850000
1.24050000		H	-5.64040000	2.50480000 -
C	7.58830000	-0.53810000	-	1.45430000
0.48750000		C	-3.87210000	1.46680000 -
H	8.51740000	-1.10540000	-	0.78730000
0.43540000		H	-4.40850000	0.53800000 -
C	6.37780000	-1.12330000	-	0.59010000
0.10540000		C	-2.49310000	1.53100000 -
			0.54840000	

C	-2.45230000	-1.33710000	-	H	-3.05570000	0.06600000
	0.55600000				5.74410000	
C	-2.04100000	-1.70870000	-	C	-1.51140000	-0.31490000
	1.84650000				4.28200000	
H	-1.23100000	-1.16670000	-	H	-0.77750000	-0.63760000
	2.33900000				5.02030000	
C	-2.66300000	-2.77790000	-	C	-1.16460000	-0.29360000
	2.49090000				2.92900000	
H	-2.34220000	-3.06760000	-	H	-0.16700000	-0.59920000
	3.49140000				2.61540000	
C	-3.69390000	-3.47770000	-	C	0.53150000	-2.67010000
	1.85100000				0.88120000	
H	-4.17770000	-4.31440000	-	H	4.20580000	2.68380000
	2.35580000				1.01270000	-
C	-4.09790000	-3.11070000	-			
	0.56480000			NiL(SCN)		
H	-4.89650000	-3.65660000	-			
	0.06290000			Ni	0.35340000	-0.03380000
C	-3.47750000	-2.04070000			0.26990000	
	0.08750000			P	-1.73670000	0.05010000
H	-3.79250000	-1.75850000			0.09160000	
	1.09250000			N	2.67350000	-3.13910000
C	-2.10370000	0.12580000			0.99280000	
	1.97190000			O	2.24980000	-0.05180000
C	-3.38320000	0.53440000			0.33060000	
	2.38360000			N	4.02640000	1.41150000
H	-4.11640000	0.87730000			0.55430000	
	1.65450000			N	1.88990000	2.22470000
C	-3.72370000	0.50600000			0.57360000	
	3.73700000			N	0.57560000	1.82050000
H	-4.71990000	0.82060000			0.57110000	
	4.04710000			S	0.21350000	-2.22150000
C	-2.78930000	0.08130000			0.12960000	
	4.68690000					

C	6.38060000	1.07040000	-	C	-3.76770000	3.84390000	-
	0.79980000				1.57770000		
H	6.44480000	2.10040000	-	H	-4.25190000	4.74750000	-
	1.15570000				1.94660000		
C	7.52840000	0.28800000	-	C	-4.52390000	2.69660000	-
	0.69670000				1.31560000		
H	8.49180000	0.71480000	-	H	-5.60120000	2.69200000	-
	0.97620000				1.47520000		
C	7.44680000	-1.03410000	-	C	-3.88830000	1.54820000	-
	0.24280000				0.84060000		
H	8.34420000	-1.64750000	-	H	-4.47620000	0.65320000	-
	0.16370000				0.63500000		
C	6.19750000	-1.55330000		C	-2.50420000	1.52720000	-
	0.11000000				0.62390000		
H	6.11400000	-2.57970000		C	-2.75230000	-1.32610000	-
	0.46980000				0.54010000		
C	5.03730000	-0.78130000		C	-2.68930000	-1.60600000	-
	0.01430000				1.91600000		
H	4.07810000	-1.20480000		H	-2.05340000	-1.00530000	-
	0.29480000				2.56910000		
C	5.12330000	0.54440000	-	C	-3.43890000	-2.65640000	-
	0.44520000				2.44530000		
C	2.68770000	1.15830000	-	H	-3.38920000	-2.87190000	-
	0.47570000				3.51210000		
C	-0.28810000	2.77450000	-	C	-4.24680000	-3.43300000	-
	0.82000000				1.60540000		
H	0.14080000	3.75760000	-	H	-4.82880000	-4.25650000	-
	1.02680000				2.01970000		
C	-1.72380000	2.67370000	-	C	-4.30540000	-3.15710000	-
	0.91580000				0.23640000		
C	-2.39050000	3.82970000	-	H	-4.93210000	-3.76140000	
	1.38390000				0.41910000		
H	-1.79780000	4.71730000	-	C	-3.55710000	-2.10550000	
	1.60650000				0.30040000		

H	-3.60100000	-1.89210000		P	-1.68590000	0.04780000	-
	1.36890000				0.42810000		
C	-2.04990000	0.13710000		O	2.28060000	-0.06980000	
	1.89100000				0.15190000		
C	-3.22100000	0.72850000		N	3.94720000	-1.48140000	
	2.39110000				0.90080000		
H	-3.95010000	1.16850000		H	4.11800000	-2.41950000	
	1.71060000				1.25120000		
C	-3.45440000	0.75620000		N	1.77770000	-2.21800000	
	3.76720000				0.85150000		
H	-4.36600000	1.21560000		N	0.50190000	-1.81340000	
	4.14890000				0.51080000		
C	-2.52050000	0.20330000		N	0.49020000	1.69630000	-
	4.64980000				0.82290000		
H	-2.70310000	0.23290000		N	1.48210000	2.36540000	-
	5.72430000				0.64610000		
C	-1.35110000	-0.38220000		N	2.39750000	3.06780000	-
	4.15500000				0.52350000		
H	-0.61920000	-0.81000000		C	6.32260000	-1.28100000	
	4.83980000				1.05500000		
C	-1.11260000	-0.41550000		H	6.33530000	-2.30810000	
	2.77930000				1.42490000		
H	-0.20130000	-0.87190000		C	7.51210000	-0.57180000	
	2.39030000				0.90870000		
C	1.68430000	-2.71080000		H	8.45510000	-1.05260000	
	0.52480000				1.16910000		
H	4.25190000	2.37880000	-	C	7.49880000	0.74420000	
	0.76790000				0.43080000		
				H	8.42930000	1.29950000	
					0.31430000		
NiL(N <sub>3</sub> )				C	6.27420000	1.33440000	
					0.10620000		
Ni	0.41540000	-0.06320000	-	H	6.24480000	2.35930000	-
	0.14520000				0.26580000		

C	5.07120000	0.63760000		C	-2.55990000	-0.58080000	-
	0.24860000				3.02160000		
H	4.13050000	1.11630000	-	H	-2.58440000	-1.61760000	-
	0.00580000				2.68420000		
C	5.08860000	-0.68660000		C	-2.89840000	-0.26960000	-
	0.72410000				4.34030000		
C	2.63700000	-1.22450000		H	-3.18180000	-1.06790000	-
	0.61650000				5.02590000		
C	-0.42160000	-2.72590000		C	-2.87780000	1.05930000	-
	0.69400000				4.77570000		
H	-0.06500000	-3.68340000		H	-3.14730000	1.30040000	-
	1.08090000				5.80430000		
C	-1.84300000	-2.62650000		C	-2.51140000	2.07970000	-
	0.46190000				3.89040000		
C	-2.58930000	-3.79270000		H	-2.49370000	3.11650000	-
	0.75930000				4.22610000		
H	-2.05830000	-4.66900000		C	-2.16850000	1.77550000	-
	1.13190000				2.57220000		
C	-3.96750000	-3.83720000		H	-1.87700000	2.56750000	-
	0.59050000				1.88390000		
H	-4.51220000	-4.74970000		C	-2.43120000	1.34500000	
	0.83080000				0.61650000		
C	-4.65200000	-2.71320000		C	-1.75210000	1.74000000	
	0.11200000				1.77950000		
H	-5.73220000	-2.73730000	-	H	-0.77840000	1.30290000	
	0.02510000				2.01100000		
C	-3.93750000	-1.55400000	-	C	-2.31610000	2.69790000	
	0.18710000				2.62540000		
H	-4.46910000	-0.67940000	-	H	-1.78490000	3.00540000	
	0.56290000				3.52610000		
C	-2.54730000	-1.49620000	-	C	-3.55530000	3.26560000	
	0.02240000				2.31000000		
C	-2.20100000	0.44230000	-	H	-3.99260000	4.01800000	
	2.12950000				2.96690000		

C	-4.23120000	2.87710000		C	-6.37830000	-1.56160000	-
	1.14800000				0.18350000		
H	-5.19260000	3.32460000		H	-6.30130000	-2.55490000	-
	0.89670000				0.62680000		
C	-3.67290000	1.91790000		C	-7.63050000	-1.05100000	
	0.30030000				0.17050000		
H	-4.19410000	1.63030000	-	H	-8.53380000	-1.63840000	
	0.61310000				0.00710000		
<b>NiL(NCO)</b>							
Ni	-0.51090000	0.04250000		C	-7.70750000	0.22800000	
	0.02340000				0.73520000		
P	1.59520000	0.06950000	-	H	-8.67310000	0.64770000	
	0.18140000				1.01750000		
O	-2.41580000	-0.05480000		C	-6.55210000	0.97630000	
	0.17670000				0.94450000		
O	-0.03220000	-4.00380000	-	H	-6.61430000	1.97300000	
	0.98300000				1.38570000		
N	-4.18670000	1.28780000		C	-5.29040000	0.46060000	
	0.82940000				0.58800000		
H	-4.40330000	2.20560000		C	-2.85220000	1.07650000	
	1.20720000				0.62690000		
N	-2.05760000	2.10460000		C	0.11820000	2.70240000	
	0.93180000				1.00750000		
N	-0.74230000	1.76130000		H	-0.31820000	3.62220000	
	0.70150000				1.40320000		
N	-0.45190000	-1.66700000	-	C	1.55610000	2.67860000	
	0.63910000				0.90110000		
C	-5.20960000	-0.82310000		C	2.21970000	3.85050000	
	0.01880000				1.33890000		
H	-4.24220000	-1.22990000	-	H	1.61940000	4.67830000	
	0.26080000				1.71700000		
				C	3.60390000	3.95880000	
					1.29660000		
				H	4.08530000	4.87280000	
					1.64290000		

C	4.37600000	2.89580000	C	3.68400000	-1.73890000
	0.81250000			0.37880000	
H	5.46200000	2.97030000	H	4.18850000	-1.33600000 -
	0.77540000			0.49930000	
C	3.74290000	1.73290000	C	4.30010000	-2.73500000
	0.37480000			1.13920000	
H	4.34450000	0.90690000 -	H	5.28790000	-3.09660000
	0.00490000			0.85410000	
C	2.34790000	1.61160000	C	3.64890000	-3.26950000
	0.41360000			2.25570000	
C	2.15850000	-0.07010000 -	H	4.13150000	-4.05020000
	1.90800000			2.84440000	
C	2.38970000	1.09420000 -	C	2.37700000	-2.80980000
	2.65780000			2.61430000	
H	2.28750000	2.07510000 -	H	1.86590000	-3.22930000
	2.19160000			3.48060000	
C	2.76170000	0.99710000 -	C	1.75460000	-1.81590000
	4.00030000			1.85650000	
H	2.94320000	1.90460000 -	H	0.75610000	-1.46330000
	4.57580000			2.12160000	
C	2.90340000	-0.25870000 -	C	-0.22330000	-2.82880000 -
	4.59890000			0.78490000	
H	3.19830000	-0.33330000 -			
	5.64590000		NiL(OCN)		
C	2.67010000	-1.42050000 -			
	3.85410000		Ni	-0.42440000	0.07880000 -
H	2.78380000	-2.40050000 -		0.01430000	
	4.31710000		P	1.68760000	0.13910000 -
C	2.29090000	-1.33050000 -		0.23650000	
	2.51400000		O	-2.29390000	-0.07010000
H	2.11480000	-2.23740000 -		0.14980000	
	1.93600000		N	-1.54820000	-3.49490000
C	2.40860000	-1.27650000		0.26230000	
	0.73770000				

## ACCEPTED MANUSCRIPT

N	-4.09830000	1.17490000		C	0.18800000	2.69460000
	0.86660000				1.05980000	
H	-4.36920000	2.08990000		H	-0.25570000	3.59370000
	1.21510000				1.49310000	
N	-1.98620000	2.05900000		C	1.62690000	2.69210000
	0.99950000				0.94270000	
N	-0.66710000	1.75590000		C	2.27890000	3.85200000
	0.73390000				1.42510000	
O	-0.38240000	-1.65310000	-	H	1.67170000	4.65940000
	0.81980000				1.83460000	
C	-4.98680000	-1.06170000		C	3.66290000	3.97370000
	0.24810000				1.38920000	
H	-3.99110000	-1.49190000		H	4.13490000	4.87810000
	0.18690000				1.77160000	
C	-6.11270000	-1.84970000	-	C	4.44670000	2.93740000
	0.00520000				0.86880000	
H	-5.97000000	-2.89830000	-	H	5.53190000	3.02320000
	0.26890000				0.83960000	
C	-7.40390000	-1.32110000		C	3.82580000	1.78640000
	0.07650000				0.38420000	
H	-8.27180000	-1.94870000	-	H	4.43430000	0.97910000
	0.12520000				0.02420000	
C	-7.56640000	0.02530000		C	2.43200000	1.65320000
	0.42460000				0.41480000	
H	-8.56400000	0.45860000		C	2.21150000	0.04200000
	0.49750000				1.97700000	
C	-6.45470000	0.82560000		C	2.56240000	1.20380000
	0.67590000				2.68290000	
H	-6.58070000	1.87680000		H	2.57470000	2.16990000
	0.94210000				2.17710000	
C	-5.15410000	0.29390000		C	2.91200000	1.11880000
	0.58610000				4.03230000	
C	-2.75990000	1.02610000		H	3.19130000	2.02210000
	0.65810000				4.57410000	

C	2.90670000	-0.12010000	-	C	-0.98870000	-2.58440000	-
	4.68120000				0.24140000		
H	3.18400000	-0.18440000	-				
	5.73370000						
C	2.54910000	-1.27800000	-				
	3.98080000						
H	2.54550000	-2.24430000	-				
	4.48480000						
C	2.19450000	-1.20130000	-				
	2.63350000						
H	1.91310000	-2.10130000	-				
	2.08790000						
C	2.48570000	-1.27000000					
	0.59630000						
C	3.73970000	-1.74460000					
	0.18080000						
H	4.23920000	-1.29700000	-				
	0.67880000						
C	4.33780000	-2.80800000					
	0.85890000						
H	5.31040000	-3.17630000					
	0.53300000						
C	3.68710000	-3.40130000					
	1.94630000						
H	4.15420000	-4.23650000					
	2.46890000						
C	2.43530000	-2.93230000					
	2.35870000						
H	1.92450000	-3.39840000					
	3.20080000						
C	1.83290000	-1.86670000					
	1.68650000						
H	0.85260000	-1.50190000					
	2.00060000						